Universidade de Aveiro
2022

Tomás Geraldo Aires

Design, analysis and testing of an innovative bi-functional blind system

Conceção, análise e teste de um sistema estore bi-funcional inovador

Universidade de Aveiro
2022

Tomás Geraldo Aires

Design, analysis and testing of an innovative bi-functional blind system

Conceção, análise e teste de um sistema estore bi-funcional inovador

Trabalho de Projeto apresentado à Universidade de Aveiro para cumprimento dos requisitos necessários à obtenção do grau de Mestre em Engenharia Mecânica, realizada sob orientação científica de Doutor Tiago Manuel Rodrigues da Silva, Investigador doutorado (nível 1), do Departamento de Engenharia Mecânica da Universidade de Aveiro, e de Doutor Victor Fernando Santos Neto, Professor auxiliar em Regime Laboral do Departamento de Engenharia Mecânica da Universidade de Aveiro.

Este Trabalho de Projeto teve o apoio dos projetos UIDB/00481/2020 e UIDP/00481/2020 - Fundação para a Ciência e a Tecnologia; e CENTRO-01-0145 FEDER-022083 - Programa Operacional Regional do Centro (Centro2020), através do Portugal 2020 e do Fundo Europeu de Desenvolvimento Regional.

O júri / The jury

Presidente / President

Prof. Doutor Pedro André Dias Prates
Professor Auxiliar em Regime Laboral da Universidade de Aveiro

Vogais / Committee

Doutor Adélio Manuel de Sousa Cavadas
Professor Adjunto do *Instituto Politécnico de Viana do Castelo*

Doutor Tiago Manuel Rodrigues da Silva
Investigador doutorado (nível 1) da Universidade de Aveiro

Agradecimentos / Acknowledgements

I would like to thank my family, orientation team, friends, and Palbit S.A.

Keywords Blind system; Window slats; PCMs; Buildings efficiency; Fast prototyping

Abstract

Nowadays, greenhouse gases are one of the main concerns for humanity. In Europe, more than 75% of the greenhouse gas emissions come from energy consumption and production. In addition, the building sector is responsible for 40% of the energy consumed. The current buildings trends is to have larger glazing areas to allow more natural light entering and raise occupants' view. On the other hand, 10 to 15% of heat losses in new buildings happen due to the glazing surfaces, so it is extremely important to improve the translucent envelope thermal efficiency.

The aim of this project is to develop a conceptual prototype of a bi-functional blind system with PCM (phase change materials) inside it slats, and to understand it thermal performance.

A conceptual prototype was mainly fabricated using FDM (fused filament fabrication) technology. It resulted in a small scaled double glazed window, composed by four glazing surfaces and five slats. Due to PCM leakage problem, it was necessary to understand the possibility of using a printed slat as macro-capsule an experimental test was done. By the end, commercialized aluminium slats were used, and sealed with high temperature silicone. A temperature monitoring system was used to analyse temperature evolution along the prototype. Several experimental tests were carried on using slats filled with PU (Polyurethane) foam and slats filled with PCM were done.

By the end, limitations were presented, but it was possible to notice the thermal improvement due to the phase change of the material. A temperature difference of -5.13% was reached the PU foam slat, when the PCM was melting. A tilting mechanism was design and suggested as future study, as long as a numerical analysis of the system.

Palavras-chave Sistema de estores; Estore; PCMs; Eficiência nos edifícios; Prototipagem rápida

Resumo

Actualmente, os gases com efeito de estufa são uma das principais preocupações da humanidade. Na Europa, mais de 75% das emissões de gases com efeito de estufa provêm do consumo e produção de energia. Além disso, o sector da construção é responsável por 40% da energia consumida. A tendência actual dos edifícios é ter maiores vãos envidraçados para permitir a entrada de mais luz natural e elevar a visão dos ocupantes. Por outro lado, 10 a 15% de perdas de calor em edifícios novos acontecem devido às superfícies envidraçadas, por isso é extremamente importante para melhorar a eficiência térmica do envelope translúcido.

O objectivo deste projecto é desenvolver um protótipo conceptual de um sistema de estores bifuncional com PCM (material de mudança de fase) dentro das suas lamelas, e compreender o seu desempenho térmico.

Um protótipo conceptual foi principalmente fabricado utilizando tecnologia FDM (*fused filament fabrication*). Resultou numa pequena janela à escala de vidro duplo, composta por quatro superfícies envidraçadas e cinco lamelas. Devido ao problema de fuga PCM, foi necessário compreender a possibilidade de utilizar uma ripa impressa como macrocápsula, tendo sido feito um teste experimental. No final, foram utilizadas lamelas de alumínio comercializadas, e seladas com silicone de alta temperatura. Foi utilizado um sistema de monitorização da temperatura para analisar a evolução da temperatura ao longo do protótipo. Foram feitos vários testes experimentais utilizando lamelas preenchidas com espuma de PU (poliuretano) e lamelas preenchidas com PCM, utilizando um forno.

No final, foram encontradas várias limitações, mas foi possível notar uma melhoria térmica devido à mudança de fase do material, e uma diferença de temperatura de -5,13% foi alcançada com as lamelas de espuma de PU, durante a mudança de fase. Um mecanismo de inclinação foi concebido e sugerido como estudo futuro, desde que se fizesse uma análise numérica do sistema.

Contents

List of Tables

Intentionally blank page.

List of Figures

Nomenclature

The next list describes several abbreviations, acronyms and symbols that will be later used within the body of the document.

Abbreviations, Acronyms and symbols

ϵ Emissivity

ABS Acrylonitrile butadiene styrene

AM Addictive manufacturing

CAD Computer-aided Design

CAM Computer-aided Manufacturing

CFD Computational fluid dynamic simulations

CJP ColorJet Printing

CNC Computerized Numerical Control

CS-PCM Core-Shell PCM

DLP Digital Light Projection

EU European Union

FDM Fused deposition modelling

g-value Solar heat gain coefficient

HVAC Heating, Ventilating and Air Conditioning)

nZEB Nearly Zero Energy Building

PCM Phase-change material

PETg Polyethylene terephthalate glycol

PLA Polylactic acid

PU Polyurethane

PVC Polyvinyl chloride

PV Photovoltaic

RTD Resistance Temperature Detector

SHGC Solar heat gain coefficient

SLA Stereolithography

SLS Selective laser sintering

SPI Serial Peripheral Interface

TES Thermal energy storage system

U-value Heat transfer coefficient

US United States of America

XPS Extruded polystyrene

Part I

Background and Technological State

Chapter 1

Background

1.1 Aim

This project aims to develop a scaled conceptual prototype of a window blind mechanism that allows the slat to rotate from -90° to +90° with the floor. The rotation allow to direct the layer where it is convenient to reduce room thermal inertia and HVAC (Heating, Ventilating and Air Conditioning) systems consumption, this conceptual prototype is developed in order the evaluate the performance of PCM (phase-change material) inside the slats.

On the sequence of the prototype development, it is necessary to design a new type of slat, composed by two layers:

- one layer full-filled with a material with high thermal resistance - insulator;
- other layer full-filled with a phase change material, which will work as thermal energy storage.

The purpose of having a slat composed by two layers and a mechanism that allows the user to select which side is exposed is:

- In winter season during the day while the building is submitted to a heat flux transfer from the inside to the outside, it will allow phase change material to charge their energy from the outside, while the insulation material, which is exposed to the interior, will prevent the heat from going outside. In the evening, the slats will tilt in, allowing the PCM to release energy to the inside to raise inside temperature to comfort temperature, while the insulation layer keeps reducing the heat transfers to outside;
- In summer, the principle is the PCM layer is directed to the outside, charging due to solar gains. In contrast the insulation layer reduces heat exchange from the outside, and, in the evening, the slats will tilt in order to change layers so that PCM can release the accumulated energy from the outside to the room. The insulation layer will decrease the heat transfer.

These two principles can be adjusted by considering the position of the room in the globe.

1.2 Background and motivation

Nowadays, greenhouse gases are one of the main concerns of humanity. The building sector is responsible for 40% of energy consumed in Europe [1]. To reduce it, governments implemented new policies. The European union's main priority is to accomplish the European Green Deal by becoming the first climate-neutral continent in the world by 2050. Energy production and use are a concern in Europe since they are responsible for more than 75% of the greenhouse gas emissions. To reduce energy production, the European Green Deal is focused on three fundamental principles: ensuring a secure and affordable EU energy supply; developing a fully integrated, interconnected, and digitized EU energy market; prioritizing energy efficiency, improving the energy performance of buildings, and creating a power sector mainly based on renewable sources [2, 3].

To improve energy performance in buildings, nZEB (Nearly Zero Energy Building) regulations were implemented. Nowadays, buildings tend to have greater glazing surfaces to allow more natural light entering and raise occupants' view, and 10 to 15% of heat losses in new buildings happen due to the glazing surfaces [4]. Therefore is extremely convenient to improve translucent envelope thermal efficiency.

Several studies were made to improve glazing surfaces thermal's efficiency, such as applying double glass surfaces filled with gases, using double window framing, or applying shading devices [5, 6].

It is relevant to understand that shading devices appeared to improve building efficiency in ancient times in desert civilizations. Besides the need to protect citizens from sandstorms and direct sunlight, the privacy necessity made people put wet pieces of clothes on the windows. This was the first time that blinds were used and it is also considered the first form of air conditioning. Later, the Egyptians modified this technique, applying river reeds instead of clothes, which was more abundant.

Later in history, between XI and XVI centuries, inspired by Persian window coverings, Venetians started to produce the famous Venetian Blinds using enslaved Persians. In 1750 these blinds were already placed through Europe, and having them was a sign of high status. Only in 1769, Edward Bevan from England patented the Venetian blind, realizing that it was possible to place wooden slats in a frame and still control the amount of light that comes inside. Later in 1841, John Hampson from the US added the feature of controlling the slats tilt angle, which is still used nowadays. In the middle of last century, vertical blinds were invented, replacing any other window covering. Late in 70 came to trend using mini-blinds due to their narrow stripes. Furthermore, in 1980 the vinyl mini-blinds replaced the aluminium ones due to their modern look. The Industrial Revolution, due to mass production, made it affordable for everyone to produce and buy window treatments [7, 8].

Nowadays, thermal energy storage systems (TES) are starting to reduce buildings' dependency on non renovated energy sources. Phase change materials are part of TES

systems that have the ability of storing and supplying thermal energy on different time needs [9]. The application of PCM in buildings envelopes will enhance the energy storage capacity of the buildings, decreasing the demand of energy consumption for heating and cooling. All this dynamic system (figure 1.1) happens passively, without the need of mechanical or electrical control. In this way, PCM can help building construction strategies to reach nZEB more easily [9].

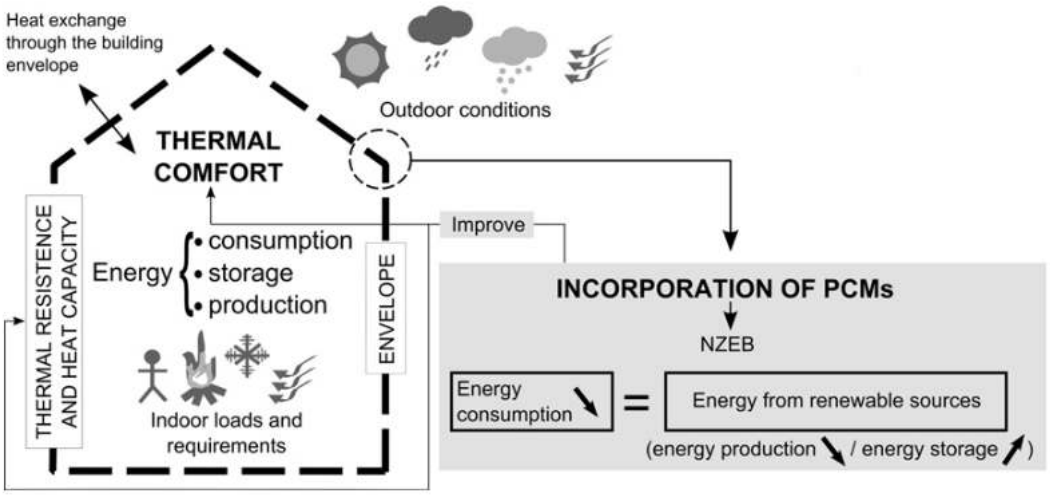

Figure 1.1: nZEB with PCM incorporated [9].

Hence the goal of improving buildings efficiency by developing windows blind systems containing PCM will contribute to a healthy and decarbonized continent by 2050.

1.3 Document placement

The document is divided in three main parts. The first part - Background and Technological state - is divided in two chapters:

- In background chapter the aims of the investigation are presented and the motivation behind it;
- In technological state chapter it is clarified the actual status of the buildings efficiency strategies and the implemented policies in EU. It is also presented the translucent envelope from a building and the shading devices associated. Additionally there is also an introduction to the thermal heat storage focused on the PCM and their applications. Finally it is presented the fast prototyping, their types and their applications.

.

The second part - Prototype development and experimental method - is divided in two chapters:

- The first chapter is the prototype development and it is presented four parts of the blind system: the slat design, the framing, the glazing and the tilting positioning;
- In the second chapter of the second part, the experimental process and results are explained and analysed in detail. The limitations of the process and possible improvements are also presented.

The last part - Conclusion - it is focused on the discussion of the achieved goals, and possible future work to do.

Chapter 2

Technological State

2.1 Buildings efficiency

2.1.1 Buildings energy consumption's

Nowadays buildings sector consumes around 40% of final energy consumption in Europe and about 30% in Portugal [10]. In 2018 the world's energy consumption was 9938 Mtoe, which raised 47 % compared with the 1973 value. Energy production is responsible for more than 75% of the EU's greenhouse gas emissions [3].

In 2018, 26.9% (516.6 Mtoe) plus 21.5% (412.6 Mtoe) of the world's electricity consumption was used for residential, commercial, and public services. Moreover, natural gas usage was about 29.9% for residential and 12.9 % for commercial and public services [11].

Besides the construction, buildings keep consuming energy for several proposals, such as: space heating, residential appliances, water heating, cooking, space cooling, lightning, and others [12].

It is relevant to acknowledge that space heating is the greatest proportion of energy consumption in residential buildings with 53% of the energy consumed by these. Hence, it is easy to understand that reducing this amount of energy is essential to improve buildings efficiency [12]. There are several ways to reach better building efficiencies to keep the buildings comfortable and safe. New architectures are allowable with new energy systems design, new construction practices, and intelligent operation of the structures after the installation is built.

Several improvements can be made to improve buildings efficiency: good building design, including passive systems and landscaping; Improved building envelope, including roofs, walls, and translucent facade; Improved HVAC systems; Thermal energy storage that can be a part of the building structure or separate equipment; Improved sensors, control systems, and control algorithms for optimizing system performance [13]. Managing energy demand from peaks periods in buildings to low demand periods using thermal energy storage might be one of the solutions to improve buildings' efficiency and reduce energy demand, providing a decrease in greenhouse gas emissions.

Building design depends on the climate where the building is placed. Around 50% of the heating load in residential buildings and 60% in commercial buildings come from flows through walls, foundations, and roofs [13].

Since the building sector was responsible for 40% of the energy consumption in Europe and 36% of the CO_2 back in 2012, the EU strategy fused on achieving a sustainable and competitive low-carbon economy by 2020 [14]. Member States were encouraged to decrease energy consumption, and instead of having buildings that are energy consumers, turn them into energy producers through retrofit measures and renewable energy sources.

2.1.2 European Union policies

The European Union established six main priorities: A European green deal, a Europe fit for the digital age, an economy that works for people, a stronger Europe in the world, promoting the European way of life, and a new push for European democracy. Focusing on the first - European Green deal - which will bring to the citizens: fresh air, clean water, healthy soil biodiversity; renovated and energy-efficient buildings; healthy and affordable food; and more public transportation. To reach European Green Deal's priority, the EU invests in several fields: climate, energy, agriculture, industry, environment and oceans, transport, finance, regional development, and research and innovation [3, 15].

Focusing on the energy field, the EU is prioritizing energy efficiency, improving the energy performance of buildings, and developing a power sector mainly based on renewable sources. The European Commission proposed the member states to renovate at least 3% of all public buildings area annually and increase the use of renewable energy in heating and cooling by +1.1% each year until 2030 [3, 16].

Nearly Zero Energy Buildings

The Energy Performance of Buildings Directive (EPBD) was implemented to promote the energy performance of buildings. In 2002 the first version was created - Directive 2002/91/EC - being updated in 2010 to the 2010/31/EU focusing on the Nearly Zero Energy Buildings (specifically found on article 9). In 2016 the EPBD directive was revised - COM/2016/0765 - to boost clean energy consumption measures and cut CO_2 emissions [17].

> "*nearly zero-energy building* means a building that has a very high energy performance,(...). The nearly zero or very low amount of energy required should be covered to a very significant extent by energy from renewable sources, including energy from renewable sources produced on-site or nearby." [1]

In other words, nZEB are energetically independent buildings or close. They are designed to increase energy performance, keeping thermal comfort to their occupants without the need of HVAC systems installation due to their construction optimization,

or they can recover to renewable energy systems to feed their demand. Although due to several climatic areas, this is not always possible. NZEB renovation combines high-efficiency technologies with renewable energy production. Renovation can mean replacing all building elements, which have a more significant impact on energy consumption. The buildings enveloping (walls, windows, roofs) provide a different energy-saving level compared to the retrofit of the building (HVAC, light systems,...) [14, 18].

2.1.3 Windows impact in buildings

To improve buildings efficiency is necessary to reduce energy losses in winter and gains in summer. It is important to look at the building's envelope. Windows and ventilation systems are responsible for 10 to 15% of heat losses (and 20 to 25% in existing buildings). Windows lose heat by conduction and convection through glazing, window frame and air leakages around window opening [4].

Windows allow sunlight to enter and heat the building. Standard windows energy transfers depend on the climate, orientation, and interior space use, although, it could be an effective part of the building climate control and lighting systems. The solar heat gain coefficient (SHGC) measures the fraction of total sunlight energy that can pass through the window. Commercially available windows can be selected from 0.29 to 0.62 values. Visual transmittance coefficient measures the fraction of visible sunlight that gets through a window, and it rounds the 0.7 value. One of the biggest disadvantages of windows is that windows transmit unwanted heat through the frame's material by conduction. So, it comes to a challenge: providing superior performance at an affordable price [13].

Nowadays, window openings can be filled with up to two window frames, where both frames are supposed to be next to the insulation's and the wall surface, forming an air gap between them. Since this option was becoming weighty for most building structures and expensive, the most used type of window improvement is multi-layer glasses (which are added to each side of the window frame) with air gaps filled with argon, krypton and others. Hence, looking for the exterior and interior of the windows is a viable way to explore and improve building energy consumption [5, 13].

2.1.4 Window blinds effect

A very common measure implemented is external shading devices since, besides shading, they allow windows to improve insulation. Shadings can be permanent or movable, automatic or manually controlled. As studied, when placed in the interior, the closest the blind is to the window, the lower the U-value of the window is, since the shading device is submitted through a convective flow. Consequently, the temperature difference between the glazing and the blind will be lower, reducing the radiation heat exchange between them and, consequently, the total U-value [19].

It is also known that the maximum impact on the U-value happens with a lower blind emissivity and when slats are closed (90°). Although, the U-value can be reduced from 8-11% (depending on the blind emissivity) when slats are open, and 14-37% if

the blinds are fully closed. Emissivity has a higher impact on the U-value when the blinds are closed due to the heat exchange by radiation with the indoor surroundings, and it can reduce as much as 60% in high standard emissivity ($\varepsilon = 0.8$). A trade-off about the placement of the interior blinds is that, if they are placed close to the window, the temperatures difference between the room and the blind will be higher, which will increase the radiation heat exchange with the room, and consequently affect the occupants' comfort [19].

2.1.5 Human interaction with window blinds

Providing occupants a comfortable and safe interior environment is the main proposal of building evolution, and new technologies have made it more accessible. Besides all the efficiency gains that HVAC systems bring, it can also provide occupants, with easier interaction, their needs, such as temperature control and inside air quality. It is also important to understand how humans interact with window blind systems. Sami [20] studied several possible interactions with the window blinds:

1. Intelligent control algorithm venetian blinds;
2. Sun protection 1 (lowered and closed when solar radiation level exceeds 50 W/m^2 outside window);
3. Sun protection 2 (same as above with threshold of 100 W/m^2);
4. Sun protection 3 (same as above with threshold of 200 W/m^2);
5. Always lowered and closed;
6. Always raised;
7. Always lowered and closed during nights (from 11 pm to 7 am), always raised at all other times;
8. Always raised when room is occupied and it is not dark (preference for view to outside).

It was concluded that a totally passive strategy (or permanently closed or always opened), a very trend common in daily life, led to the most energy consumption option. By that, it is important to notice that in the heating season, to improve buildings' efficiency, raising the blinds will allow the sun heat, and lowering and closing the blinds at night will prevent the heat to go outside [20].

It is plausible that improving window blind systems using bi-functional slats filled with PCM and thermal insulation will be more favourable to human usage and enhance the window U-value.

2.2 Translucent envelope

Building's translucent envelope can be separated into two components: the glazing surface and the shading devices. Shading devices technologies were divided in different groups (figure 2.1). It was made a distinction between fixed and movable systems. The four main groups of movable systems that were created: roller blinds, vertical blinds, venetian blinds, and others.

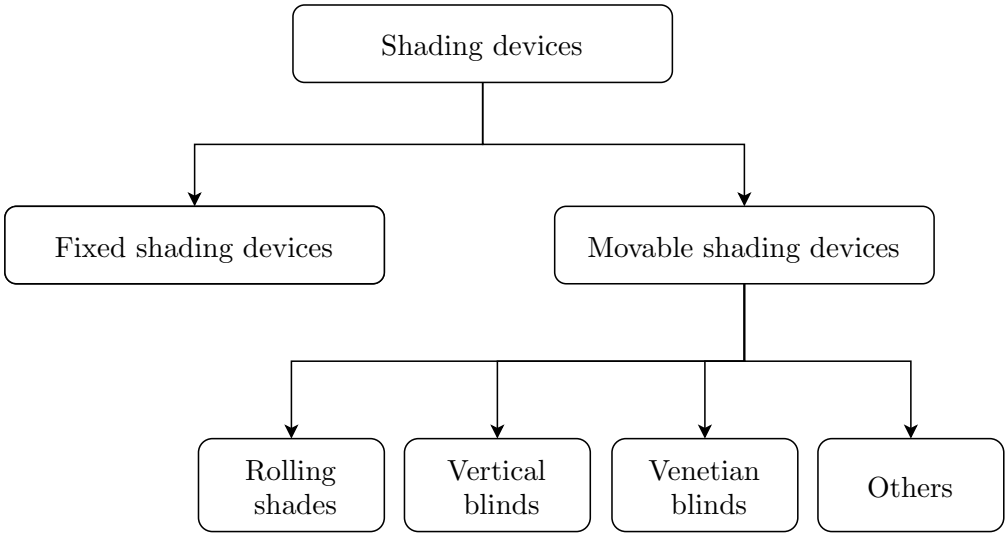

Figure 2.1: Window treatments types

2.2.1 Glazing

Glazing surfaces, in new buildings, are rising in size to increase natural light inside the buildings. As previously said, windows are responsible for 10 to 15% of heat losses in buildings. Besides simple glass solutions with different thicknesses, multi-layer glass and double framed glass are other possibilities to decrease heat transfer fluxes. Although it still cannot reach the thermal resistance value of building walls [5].

Simple glazed solutions (figure 2.2a) have six times lower thermal resistance than walls and roofs [21]. Double framing (figure 2.2b) is a commonly used solution since one of the frames is placed close to the outside surface, near the insulation layer of the wall, and the other frame is placed near the inside wall surface. The distance between them creates an air gap which works as heat insulation. When the sun hits the glazing surface directly, the greenhouse effect happens, and air temperature in the gap can exceed the indoor temperature increasing the heat flux to the inside. Comparing with a simple framing with single glazing, an increase of 130% of thermal resistance is noticed. Besides higher cost, another disadvantage of double framing solutions is that the U-value of the frame is higher than the glass, so that it will increase heat losses in windows by conduction [5, 22].

A multi-layer glass system (figure 2.2c) adds more glazing surfaces to a simple one. By fitting two layers with 4 mm thickness, two air gaps are being created, and it is possible to decrease heat losses through the window by 56% [5]. Vacuum glazed solutions were replaced by vacuum glazed filled with inert gas (argon, krypton, or xenon) to reduce pressure and stresses between the glass layers [21]. A disadvantage of multi-layer glass is that three or more layers of glass are too heavy for most conventional building structures [13].

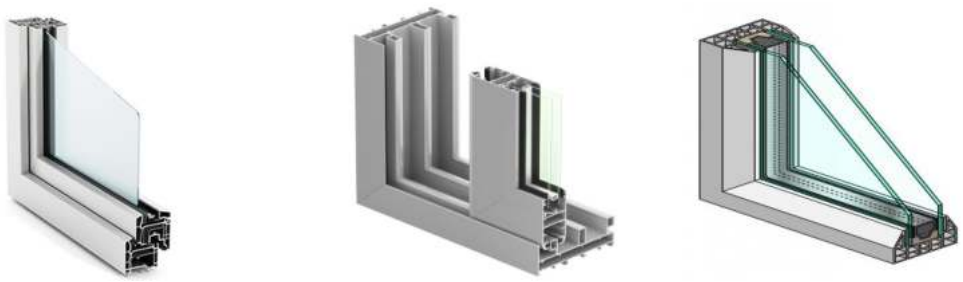

(a) Simple glazed [23] (b) Double framing [24] (c) Multi-layer glass [25]

Figure 2.2: Glazing types

2.2.2 Fixed shading devices

Fixed shading devices can be found inside or outside of a translucent envelope. These shading devices are used to control solar radiation inside the building, increasing visual comfort, and decreasing glare. It can also be prejudicial to the building since it can increase the need of artificial lighting when it is not needed. Due to that, it is crucial to find the proper place to build them [26].

Overhangs

The most common fixed shading devices are overhangs (figure 2.3a). It is a surface placed over a window, on the outside, providing shade. The shading shape and size is dependent on the sun's position [26].

Horizontal and vertical louvers

Horizontal louvers (figure 2.3b) are designed to prevent high summer sun from going inside and allow low winter sun to enter the interior during the heating period. Louvers' dimensions depend on the distance between them, the place and climate where the building is located. Its size also influences the cost. As it is built to catch direct sunlight, the louvers' top face should have light colour to reflect natural light. Vertical louvers (figure 2.3c) are more effective on east and west facades, and, besides creating a shade, it also works as a windbreak. Vertical fin can also be adjustable with the sun's location, and when oblique to the wall, it creates an asymmetrical shading mask [26].

Egg-crate

Egg-crates (figure 2.3d) is the most complex from the fixed shading devices since it has both vertical and horizontal shading elements, blocking solar radiation from all directions, being extremely efficient. On the other hand, they block solar gains in winter, view range, and natural light [26].

Others

Other buildings, and trees are considered as fixed shading devices [26].

(a) Overhangs

(b) Horizontal louvers

(c) Vertical louvers [27]

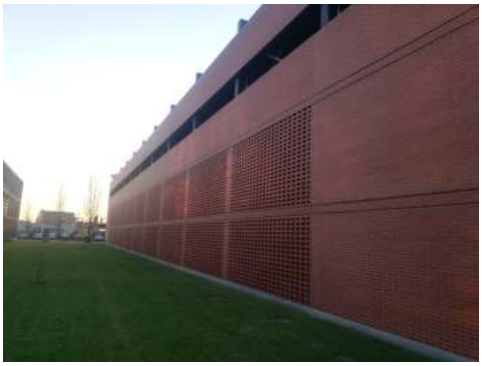

(d) Egg-crate

Figure 2.3: Fixed shading devices

2.2.3 Movable shading devices

Rolling shades

Rolling shades (figure 2.4) are mainly used for glare control, and besides manual controlling, they are also founded with motorized solutions. They can be found in several types: roller shades, solar shades, night and day shades, *corti* glass shades, zipscreen shades, ziptrack shades, and roller shutters.

Roller shades

Roller shades (figure 2.4a) are mainly used as an internal shading device and are composed of a screen usually made of fabric. This fabric screen is linked to a horizontal bar on the top of the glazed part. The bar is directly connected to a motor or a string, depending on the type of controlling system. The bar will roll, and the screen will roll itself with the bar, rising and allowing direct sunlight to enter.

Night and day shades

Night and day shades or zebra shades (figure 2.4b) are internal shading devices. They are known because they use a 2-in-1 combination of light filtering and blackout fabrics allowing natural light to enter and still provide privacy. They can also be found with a cordless system and cellular profile.

Corti glass shades

Corti glass shades (figure 2.4c) are internal shading devices that work similarly to roller shades, but they are individually adapted to each part of the window or door. Usually they are used to control the glare and luminosity of the room.

Zipscreen and ziptrack shades

Zipscreen and ziptrack shades (figure 2.4d) are both external shading devices with similar working principles. Usually, these systems are placed on a terrace. Besides being used as shading devices, they can provide comfort in different weather conditions such as rain and wind due to their resistance and waterproof screen. The main difference between the two devices is on how the zip tracks cover the screens.

Roller shutters

Roller shutters (figure 2.4e) are a widespread solution as a shading device, usually applied on the exterior side of the glazing surface. This system is composed of hinged blades linked to a tube where the blades curl around. The blades can be found in different sizes and are made of PVC or aluminium, and they provide high security when talking about ember from fires. Besides that, these are usually filled with an insulator (mainly polyurethane foam) to raise the system's thermal and sound resistance. This system is also used for doors and gates as a protective system from intruders. They allow the user to control them up, allowing occupants to enjoy a full view, and letting direct sunlight enter, or, when almost entirely close, diffuse sunlight providing comfort reducing artificial light. The system can be operated manually, or by motor and with rechargeable battery [28, 29].

Pinoleum shades

Pinoleum shades (figure 2.4f), also known as plantation blinds, are commonly used as an internal shading device. Plantation blinds can decrease glare and block some UV radiation. It allows the room's occupant to see to the outside, even when the system is down, but on the other hand, on the other hand, they are effective in privacy since it blocks the view from the outside. Nowadays, they are mainly made of woven [30].

Vertical Blinds

Vertical blinds (figure 2.5) are commonly used in commercial and residential buildings. They can be found in different types: curtains, panel blinds, vertical blinds, shutters and venetian blinds.

Curtains

Curtains (figure 2.5a) are internal shading devices made of fabric usually held by a horizontal bar placed above the window, which allow the user to move the curtain from side to side in order to allow direct daylight to enter. They can provide privacy and, when placed to the side, provide a complete view from the glazing part of the building.

Panel blinds

Panel blinds (figure 2.5b) are also internal shading devices composed by several vertical panels, usually made of fabric. The user can move them to the side, allowing direct sunlight to enter.

Vertical blinds

Vertical blinds (figure 2.5c) are composed by vertical louvers, usually made of fabric or PVC (polyvinyl chloride), and are mainly used as an internal shading device. They can be moved to the side, allowing direct sunlight to enter, or, when closed, preventing glare but allowing diffuse sunlight to enter.

Shutters

Shutters (figure 2.5d) can be applied internally and externally. They can be made from wood, PVC, or aluminium. They can be opaque, and the only way to control the sunlight intensity that enters the rooms is by opening them to the side, which means that it is fully opened or fully closed.

Venetian blinds

Venetian blinds' are composed of slats equally displaced, and occupants, besides controlling their height, can also control their tilt angle. They are efficient in blocking direct sunlight and reflecting it to the inside. Direct sunlight passes to the inside without

(a) Roller shades [31]

,,

(b) Night and day shades [32]

(c) Corti glass shades [33]

(d) Ziptrak shades [34]

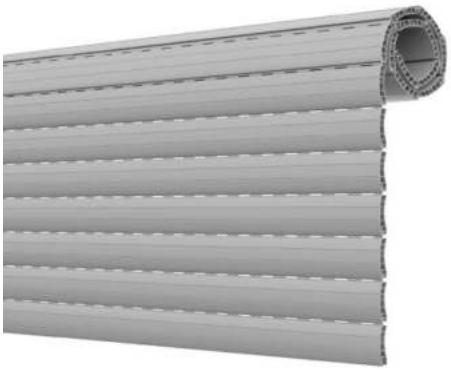

(e) Roller shutters [35]

(f) Pinoleum shades [36]

Figure 2.4: Rolling shades

(a) Curtains [37]

(b) Panel blinds [38]

(c) Vertical blinds [39]

(d) Shutters [27]

Figure 2.5: Vertical blinds

hitting the slats. The remaining sunlight passes indirectly by reflection after hitting the slats, and the diffuse radiation, which the slats can disperse, remains diffuse. Their shading and viewing factors can be easily adjusted by changing the tilt angle, providing privacy and an acquirable view, besides the visual comfort to the room occupants.

Thermal performance are dependent on several factors: tilting angle, height adjustment, the distance between slats, number of slats, slats characteristics (shape, size, color, material), and solar angle of incidence. Venetians' blinds are found in several types: standard venetian blinds, micro blinds, macro blinds and integral blinds [40, 41].

Working principle: Standard venetian blind slats can be opened or closed using a tilting chord or wand due to the tilt mechanism. Besides that, another chord, when pulled up or down, raises or lowers the slats respectively due to the cord lock mechanism. The tilting chord or wand is connected to a worm gear that is connected to a headrail. The headrail is linked to the slats by several drums and string ladders (depending on the length of the slats). Rotating the wand or pulling the chord will turn the motion to the slats. The lift strings are used to control the height of the slats. They go to the top box, pass the cord lock mechanism, and go back down, passing through the middle of the slats until the bottom one. The string number varies with the length of the slats to prevent unbalanced slat lifting. The lock mechanism is composed by two rollers to lock these strings, and when pulling the strings aside, these rollers will pinch the strings. When the string is pulled to the opposite side, it will release the textured roll and afterward the strings, allowing the slats to move up or down.

Slat shapes: Nowadays, there are two types of slats profiles. Curved-shaped slats, which are sub-divided in equally curved or C profiles, that are the most of the slats currently produced, and provide an 0° to 180° tilting angle range. The second type is concave curves or Z profile, which allow full darkness but only have a 0° to 90° tilting angle range [29, 42].

Standard blinds, micro blinds, and macro blinds: Standard blinds, micro blinds, and macro blinds can be fitted as an internal or external shading device. The difference between micro, macro, and standard venetian blinds is the slat size. A standard blind slat is $25mm$ wide, macro blinds slats are $50mm$ and are more used in large windows or glazing surfaces, and micro blinds slats are $12{,}5mm$ wide, which can provide more privacy and do not let enter so much light as the previous (figure 2.6a).

Integral blinds Integral blinds (figure 2.6b) are a recent solution, which is placed between a double-glazed surface. These systems are mainly applied in bifold doors but can also be placed in windows. They have all the benefits of a venetian blind, such as slat tilting angle control to control the viewing factor and the amount of direct and diffuse natural light that goes inside. Since they are in between the two-glazed surfaces, they are not exposed to accidental damage, safer for children and pets, and permanently clean.

Their tilting and lifting mechanisms have similar principles as conventional venetian blind, where they can be found with a cord system or an automatic solution. Additionally, there is a patented feature based on a magnetic device encapsulated in the window frame and a magnetic slider in this system. Integral blinds can also be made with cellular shades technology [43, 44].

(a) Standard venetian blinds (b) Integral blinds

Figure 2.6: Venetian blinds [27, 43]

Other window treatment systems

Roman shades

Roman shades (figure 2.7a) are used as internal shading devices. Commonly they are made of fabric, and can only be adjusted upwards and downwards, controlling the direct and diffuse sunlight that enters. When opened, these blinds stack up evenly, and when closed, they can cover the full window, always letting some natural light enter.

Cellular shades

Cellular shades (figure 2.7b) , also known as honeycomb shades, can be used as an internal or external shading device. Due to several fabric's solutions, from light to opaque filtering, cellular shades provide several light control options, blocking direct sunlight and allowing diffuse sunlight. Furthermore the air gap inside them, they can provide high thermal resistance to decrease heat fluxes. Another advantage of cellular shades is the stack size, which can become quite thin. Honeycomb shades can be presented with and without cord systems, which aesthetically can be a benefit [45].

Deciduous plants

Deciduous plants (figure 2.7c) are useful when placed next to a window since they work as a dynamic shading device, adapting to the seasonal period. In the warm season,

their leaves can provide shade to the glazing, decreasing the heat flux to the inside. In the cold season, as they do not carry leaves, the sunlight and the heat flux can pass to the inside of the glazing, providing comfort to the room's occupants.

Shoji blinds

Shoji blinds (figure 2.7d) , also known as Japanese panels, and are originally from China. They are used in the transition between the inside and the outside. Traditionally they are made with a bamboo structure and *Washi* paper. Besides blocking direct sunlight and allowing diffuse natural light to enter the room, they can reduce the glare and work as an air filter due to the paper's microporous structure [46, 47].

Mosquito screens

Besides preventing the insects to go inside the house when the windows are opened, Mosquito screens (figure 2.7e) can prevent direct sunlight from entering and reduce glare. Mosquito screens can be an advantage since they can be applied with other shading devices.

Blind awnings

Blind awnings (figure 2.7f) are external shading devices used to block direct sunlight to decrease heat flux to the interior. They come equipped with a retractable mechanism that allows the user to control the awning size [48].

Overview table

In table 2.1 can be found an overview of the most relevant types of shading devices for the project itself, and their features.

2.2.4 Window blinds as a source of energy

To reach a more efficient building, it is needed to take advantage of each part of the building. Electrical and thermal energy (section 2.3), are two types of energy that have been studied to take advantage of window treatments.

Electrical energy

A solution to reach nearly nZEB through shading devices is by taking advantage of renewable resources. A blind system equipped with photovoltaic (PV) cell as seen in figure 2.8.

PV blinds are venetian blinds, with the photovoltaic cell through their slats. Likewise blocking direct sunlight and allowing skylight to hit, these blinds can generate electric power. Studies have been made to optimize power generation and still allow the skylight pass to the interior [41].

These cells have been applied in two different systems:

(a) Roman shades [34]

(b) Cellular shades [49]

(c) Deciduous plants [50]

(d) Shoji blinds [51]

(e) Mosquito screens [52]

(f) Blind awnings [53]

Figure 2.7: Other window treatment systems

Table 2.1: Shading devices overview

	internal application	external application	U-value $[W/m^2K]$	lightning control [Yes/No]	darkness [Yes/No]	privacy [Yes/No]
roller shutters [26, 54, 55]		x	0.3-1.3	Yes	Yes	Yes
vertical blinds [26, 54]	x			Yes	No	Yes
venetian blinds [40, 42, 54, 56]	x	x	2.49-2.63	Yes	No	Yes

1. Uni-directional blind system – PV blind is orthogonal to the profile angle of the sun to maximize the potential energy efficiency of the cells, ignoring the interior light ;
2. Bi-directional blind system – PV blind blocks direct sunlight and allows incoming skylight to minimize shading effect.

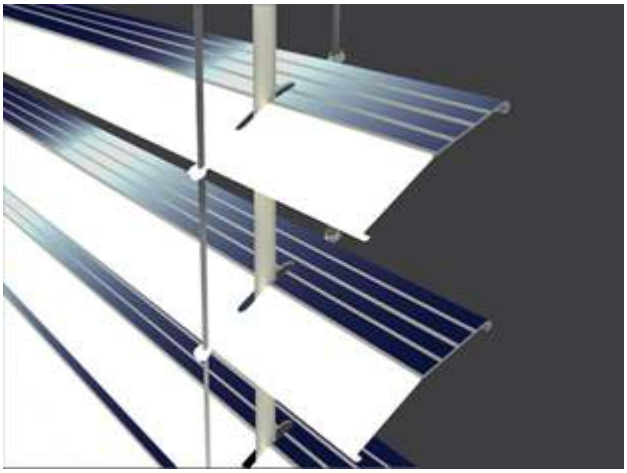

Figure 2.8: Photovoltaic cells applied in window slats [41]

Studies show that a bi-direction blind system reached higher power generation through PV blinds and more lighting energy savings due to the inside luminous environment. Although these systems are still in the research stage, the shading effect request is still a challenge since it has a great impact on PV cells performance [41].

2.3 Thermal heat storage materials

Thermal energy storage (TES) materials are part of the called intelligent materials, which respond to external stimulus, such as stress, light, pressure, moisture, temperature, pH or electric/ magnetic fields. TES materials are capable of absorbing heat and, later with the change of temperature, release it [57]. The main advantage of TES materials is the fact that they can contribute to supply energy demands that do not coincide in a time interval [9]. They can store and release energy depending on the size and the phase of the material. Their passive way of working is also a benefit since they do not need any mechanical system to work. The TES materials can be divided by the type of thermal energy stored (figure 2.9), which can be sensible, thermochemical, or latent heat.

- **Sensible heat storage** corresponds to a change of temperature of the materials, and the amount of energy stored is mainly dependent on the density, specific heat, among others. Hence, it is necessary a huge amount of resources to store a notable amount of energy, which is a disadvantage. Examples of sensible heat storage: Water, oil-based fluids, molten salts, rocks and metals. Since, for example, water is corrosive to other materials, it is needed to store it apart, which means heat loss over time [57].

- **Thermochemical heat storage** is the use of exothermic and endothermic reactions which can result in a material. For example, in sorption processes where a gas reacts with a liquid or solid material. Additionally, these materials have a low heat losses and a high heat storage but it is not common in real application due to the complexity of the process, price, toxicity and safety. [57].

- **Latent heat storage** materials, mostly known as phase change materials, change their phase when storing energy. Compared with sensible heat storage , it can be considered a better solution since it requires less volume of materials to get acceptable energy efficiency. When kept at a constant temperature, these materials can avoid corrosion processes. PCM can be split into three main types: Inorganic, Organic and Eutectic, which will be explained in section 2.3.1.

2.3.1 Phase change materials

Phase change materials - PCM - change their phase during the energy storage process acting almost as an isotherm reservoir of heat. When temperature increases, PCM change phase from solid to liquid absorbing heat due to this endothermic reaction. When the temperature decreases, they change phase from liquid to solid, releasing heat due to this exothermic reaction. Understanding the principle of PCM is very simple, although evaluating their performance when applied to a building is still a challenge [9].

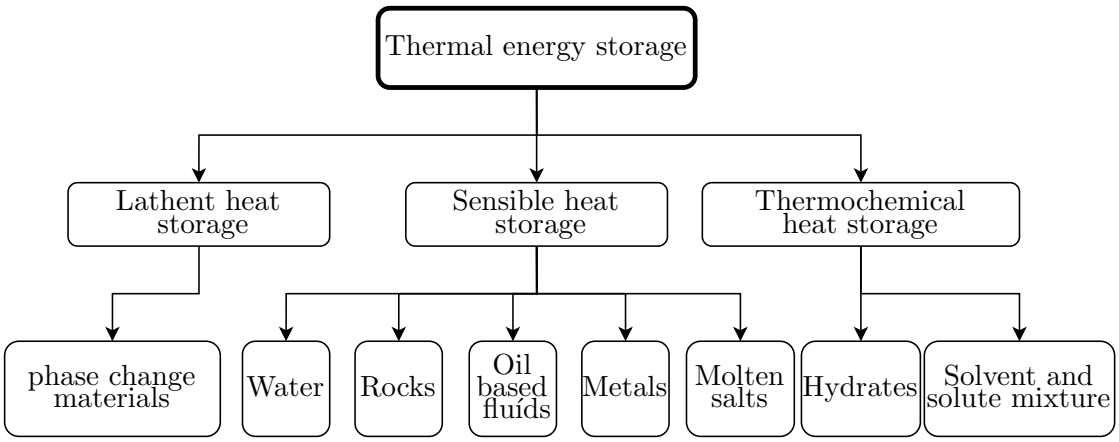

Figure 2.9: Thermal energy storage

Advantages and disadvantages

PCM can be divided into three main groups: Inorganic PCM, Organic PCM and Eutectic PCM. The advantages and disadvantages are presented in table 2.2.

Encapsulation types

Encapsulation or Core-Shell PCM (CS-PCM) (figure 2.10a) is a process of shelling the PCM with a suitable coating material to keep it isolated from surrounding. Encapsulation ensures the sustainability of PCM composition, which can be changed by connection with the surrounding. It improves thermal and mechanical stability and heat transfer rate [58].

Encapsulation classification is defined by the size of the capsule. A capsule with a diameter lower than 1000 nm is a **nano** capsule, capsules from 1 mm to 100 mm is a **micro** capsule and greater than 1 cm is a **macro** capsule [59].

Generally nano-encapsulation and micro-encapsulation processing techniques tend to be more complicated and expensive when compared with the macro-encapsulation since the capsule size is smaller. However, reducing capsule size provide to particles higher structural stability and better fracture resistance. The above mentioned methods have an inherently low thermal conductivity due to the shell material. [59].

Macro-encapsulation besides being an easier process of encapsulation, can also provide more flexible choices of PCM and shell material selection. Although to reach optimum performance, correct selection of PCM and shell materials needs to be done [59]. Cabeza et al [60] studied the behaviour of a water tank containing a PCM module made of aluminium with 1.5 L capacity. This module was filled with PCM-graphite compound due to its high heat transfer rate with a thermal conductivity of 2 to 5 W/mK.

It is important to consider the selection of the shell material since it differ with the temperature range needed, the thermal conductivity, encapsulation process, permeability, toxicity, compatibility with the core and the surroundings where it is going to be

Table 2.2: PCM advantages and disadvantages [9]

	advantages	**disadvantages**
organic	high energy storage	low thermal conductivity
	good chemical stability over time without segregation	possible instability at high temperatures
	fatty acids and alcohols come from renewable sources	PEG and paraffins come from non-renewable sources
	availability in a large temperature range	lower volumetric latent heat storage capaciety
	high latent heat of fusion (fatty acids have high heat of fusion values comparable to that of paraffins)	lower density
	freeze with little or no supercooling	non compatibility with plastic containers
	congruent phase-change	more expensive (commercial paraffins are cheaper and more available than pure paraffins and fatty acids are 2-2.5 times more expensive than tecnhical grade paraffins
	self-nucleation properties	relative large volume change (however some fatty acids could undergo small volume changes flamability
inorganic	almost double thermal storage capacity comparing to organic PCM	salts can present incongruent fusion and precitation
	high thermal conductivity	possible dehydration of the salts
	predictable and thermally and chemically stable	poor nucleating properties and supercooling problems
	low vapour pressure in the melt form	incongruent melting and dehydration in the process of thermal cycling
	not dangerous , non reactive and non corrosive	phase segregation during transition and thermal stability problems
	compatibility with conventional material of construction	their application could require the use of some nucleating and thickening agents
	recyclable	decomposition and phase separation
	higher volumetric latent heat storage capacity i.e higher melting enthalpy	non-compatible with some building materials
	higher latent heat of fusion	corrosive to most metals and slightly toxic
	low cost and readily available	
	sharper phase-change	
	higher thermal conductiviy	
	non-flammable	
	lower volume change	
	compatible with plastics	
	it is better to use slat hydrates than paraffins to reduce the manufacturing/ disposal enviornmental impact	
eutectic	they merge and solidify congruently avoiding segregation	same disadvantages as the pure organic or inorganic PCM
	adjustable phase change temperature by mixing different materials	limited data are available on their thermophysical properties
	sharp melting temperature (could be used to deliver the desired melting temperature required)	some fatty eutectics have quite strong odour and therefor they are no recommended of use as PCM wallboard
	volumetric thermal storage density slightly above organic compounds	
	no segregation and congruent phase change	

incorporated. CS-PCM can be found in several container shapes as cylindrical, tubular, spherical or rectangular[58]. The main advantages and disadvantages can be found in table 2.3.

Shape-stabilized PCM (figure 2.10b) is another method to keep PCM. It is a composite where the PCM in its molten phase is mixed with another material (generally porous) by capillarity. This method can be considered cheaper since the support materials can mainly be found in natural occurring porous materials[57]. The main advantages and disadvantages can be found in table 2.3.

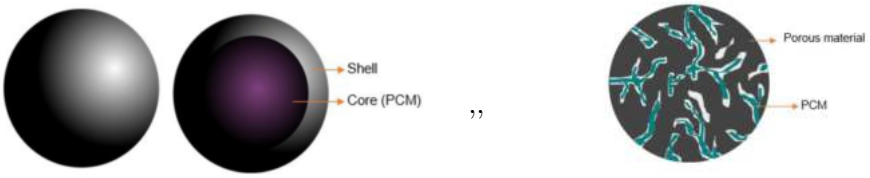

(a) Core-Shell PCM (b) Shape-stabilized PCM

Figure 2.10: Encapsulation methods [57]

Table 2.3: Encapsulation types - advantages and disadvantages [57]

	Advantages	Disadvantages
CS-PCM	High surface area for heat transfer Reduce reactivity with the surrounding, less corrosion Control of volume change during the phase transformation Small particle size that could make more efficient the system	Expensive process and reagents Must obtained a non-permeable capsule to prevent leakage Some methods for production can present harmful by-products Many steps to be produced PCM can diffuse to the surface and gradually be lost if the process is not optimized
SS-PCM	Cost-effective production process Large particle size, it may be easier to handle for certain applications Porous materials are found in natural inorganic supports Hierarchical porosity can be obtained by templating methods May increase thermal conductivity Few steps for the production Different morphologies can be achieved as fibers, amorphous particles or rounded particles	Limit in the amount of PCM that can be contained Is difficult to obtain nanoscale particles More contact between the PCM and the surroundings, leading sometimes to corrosion or not desirable reactions

2.3.2 PCM applications

Nowadays PCM can be found in several applications such as:

- Domestic hot water [61];
- Heat transfer systems [62];
- Solar thermal power plants [63, 64];
- Peak load shifting - cold storage systems (chilled water, ice storage and eutectic salt) use PCM to shift electrical peak load [62];
- Industrial applications - food packaging, fermentation processes, food preservation [62];
- Transport of temperature-sensitive materials and air-conditioning systems [62];
- Thermal insulation for functional fibers [62];
- Buildings envelops [62];

PCM in buildings envelopes

Nowadays, PCM can be found in the buildings' envelopes. In opaque envelope several studies have been done using PCM as the external, middle or internal layer of a wall, in roof systems, floor heating systems, bricks filled with PCM and PCM enhanced wallboards [9, 62, 65–67].

In the translucent envelope, several studies were found, such as double glazed windows filled with water, paraffin or eutectic PCM, window film composed by PCM, PCM applied in vertical slats, PCM applied in aluminium window shutters [68–70].

Vertical blinds with PCM: Helmut et al. [71] was monitoring a vertical blind filled with PCM from winter of 2008 until the summer of 2010. The study aimed to understand if the application of PCM in blind systems could decrease the temperature peaks.

The prototype was developed by *Warema®* (a leading manufacturer of sun shading systems in Germany), and the *Delta – Cool 28 PCM* was used, which is a salt hydrate with a melting range between 26℃ and 30℃ and with an enthalpy of $188\,\mathrm{J\,g^{-1}}$ produced by *Dorken®*. This company also encapsulated a hollow polycarbonate blind with a 12 mm gap filled with the PCM and sealed it at the ends. So, in this study conditions, $1m^2$ of the blind area contained about 17 kg of PCM. All the slats were filled with highly reflective white fabric to ensure good sun protection performance, resulting in a final slat thickness of 15 mm (figure 2.11).

In order to get g-values, a test cell composed of two temperature-measure chambers was used. The window was exposed to an irradiance of up to $530\,\mathrm{W\,m^{-2}}$. In stationary condition (fully closed), after 24 hours, the PCM blind reached 35℃, while the glass reached 42℃, and the g-value of the system went from 0.25 to 0.35 when the PCM was

melted. The PCM storage time was about 12 hours. When the slats were tilted 45°, the g-value went from 0.3 to 0.41 when melted.

The study was made in four offices, two located in Karlsruhe with the windows oriented westward and two located in Kassel, with the windows oriented southeast. The office rooms were occupied by two people and contained typical office equipment. The conventional blind had a solar reflectance of 0.8, and the PCM-blind had 0.78.

In Karlsruhe offices, due to the window orientation, the direct sun incidence increased the operative room to a maximum of 32℃, and in the room with a PCM-bind to 34℃. In the "after-work" time, the office rooms reached 31℃ in the PCM-blind and 33℃ in the reference room.

A long-term analysis showed that PCM were never completely melted if they could not be regenerated the night before. Thus four-day monitoring was made and it was noticed that although the outside temperature dropped to 14℃ in the nighttime, the PCM never dropped under 26℃. This means that PCM could not be fully regenerated during the night. During same nights, the same parameters were measured in a PCM-blind with a ventilation system, where the PCM dropped to 22℃. It was concluded that the full regeneration of the PCM can only be reachable using ventilation systems and tilted windows combined.

In Kassel, during winter analysis, the PCM was able to store the energy that came from direct solar radiation and kept the temperature above 20℃ for several hours, which contributed to the thermal comfort of the occupants.

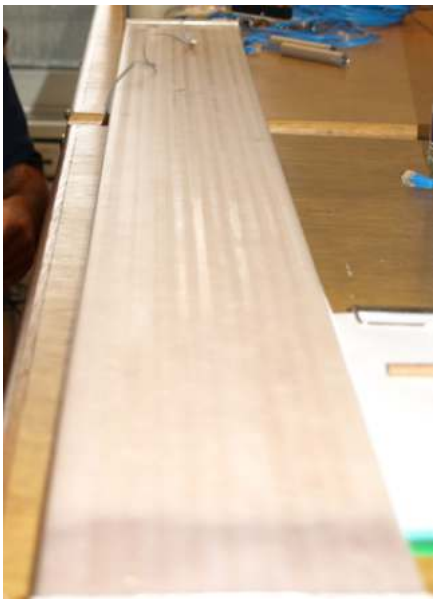

Figure 2.11: Vertical blinds filled with *Delta – Cool 28 PCM* [71]

Similar experimentation was made by Michal et [72], where an evaluation of the energy efficiency of an internal vertical blind containing PCM was made.

The window blind was made of 12 vertical aluminium profiles covered with black matter paint, and each slate was sealed using epoxy resin *Epidian 6* with hardener Z1. The reference blind was filled with extruded polystyrene (XPS), and the other was filled with a PCM (figure 2.12).

The chosen PCM was RT28 which is a mixture of paraffin, produced by *Rubiterm GmbH* ® with a solidification temperature at 21℃. Ciech produced the matrix, and it was composed by Osakryl OB copolymer.

The chamber, placed in Rzeszów, was composed by two identical glazing systems oriented to the south side, and it is fully insulated with a $20cm$ layer of mineral wool on the other orientations. Each compartment was equipped with an independent oil heater connected to its energy consumption meter. Measurements were taken each 10 minutes.

A reduction in the temperature peak of around 10℃ on the inside glass temperature in the chamber part with PCM was noticed. The heat flux during a sunny day was also reduced in the PCM blinds in around $100\mathrm{W\,m^{-2}}$. During the night after a sunny day, it was also possible to notice a change in the trend of the heat flow from the blinds with PCM when the temperature of solidification was reached. Regarding energy consumption needed to power oil heaters, it was presented that the PCM blind part was lower by 7.8% than the reference part.

Figure 2.12: Vertical blinds filled with *RT 28* [72]

PCM in window shutters: Silva et al. [73] evaluated the performance of a window shutter filled with phase change material under summer Mediterranean climate conditions.

A test chamber, built by *COMOD®*, was used, and it was placed in Aveiro (figure 2.13). The translucent facade was south oriented. The structure was made of galvanized steel profiles, and it was insulated with 40 *mm* of polyurethane foam on the walls and 80 *mm* of fibreglass on the roof. The cell was divided into two compartments by XPS insulation, and the floor was composed by *Phenolic Frame*. The translucent facade was composed of double glazing windows, and the window shutter system was placed in the interior.

The only difference in each part of the chamber, were the slats: either aluminium hollowed slats or aluminium hollowed slats filled with paraffin *PCM RT28HC*. The PCM was provided by *Rubitherm ®* and had a melting temperature range that goes from 27℃ to 29℃ and is chemically inert and does not suffer the supercooling effect (phenomenon that the liquid does not solidify or crystallize, even its temperature is lower than the freezing point, which limits the usage of PCM [74]). It also has a good life cycle assessment. The aluminium hollowed slats were selected since it is one of the most used materials for window shutters in Portugal, and their thermal conductivity enhances the PCM phases.

One of the first challenges found was the slat sealing. Mounting glue, liquid metal, high-temperature epoxy glue, polyurethane glue and high resistant glue were tried. The combination of silicon and epoxy glue was the final decision applied to the prototype.

During the monitoring phase, the outside temperature ranges between 13.2℃ and 24.7℃ and the solar radiation between 237W m^{-2} to 306W m^{-2} with an individual maximum peak of 1200W m^{-2}. The wind was also considered, and it was interfering 24% of the time and varying between 3m s^{-1} and 6m s^{-1}.

Inside the reference compartment, the temperature reached the maximum temperature of 48℃ and the minimum temperature of 14℃. While inside the PCM compartment, the highest temperature reduced by 22% and the lowest temperature increased 18%. It was noticeable that during the monitoring days, the PCM shutter reduced 6% the maximum temperature and increased by 11% in the minimum temperature compared to the reference. The PCM shutter is also influenced by the time delay reaching the highest and lowest temperature.

2.4 Fast prototyping

The term "fast prototyping" was the first referring to the possibility of having physical models directly from digital information and being fabricated by layer technologies – addictive manufacturing (AM)[75]. AM existed for over 30 years, but only after 2009, when the last major pattern for fused deposition modelling (FDM) expired, printers could be produced without infringing on intellectual property capturing the interest of public and technology experts [76]. The term fast prototyping could include both subtraction process (CAD/CAM/CNC) and addiction processes (fabrication by layers).

Figure 2.13: Window shutters filled with *PCM RT28HC* [73]

With the time and with the normalization of 3D printing, this term started to refer only to the fabrication process by layers [75].

2.4.1 Advantages and disadvantages

The main advantages of 3D printing process are: the automatic and low vigilance process, which is safe for the user to let it print; the capability to produce three dimensional models which are complex and detailed; the fabrication of models with encapsulation on the interior of the surrounding surfaces, which would be impossible using subtractive processes; the reduction of delivery time of exclusive parts (no moulding or jigs are needed); The equipment's are clean and not noisy which allow them to be installed out of industrial shop floor as offices or ateliers [75].

The main disadvantages are: the low printing speed, depending on the precision, detail and dimension of the model; the working volume of the machine usually is reduced (in the most conventional machines it is limited to 300x300x300 mm^3);The diversity of available materials is still reduced, although it has been increasing; The resultant surface might need coating for finishing; The 3D printed parts in several materials are structural less consistent and resistant comparing to other processes as machining or casting [75].

2.4.2 3D-Printing technologies

Nowadays there are a lot of 3D-Printing processes existent in the market, such as: SLA (Stereolithography), DLP (Digital Light Projection), FDM (Fused filament fabrication), SLS (Selective laser sintering) , Solidscape (DoD process), PolyJet (Multi-Jetting Modelling) and CJP (ColorJet Printing), that are presented in table 2.5.

The three most commonly used printing materials in FDM printers are PLA (polylactic acid) , PETG (polyethylene terephthalate glycol) and ABS (acrylonitrile butadiene styrene). In table 2.4 a comparison between those materials was made.

Table 2.4: FDM process - materials comparison [75].

Property	**Lower**	**Medium**	**Higher**
Ecologic	ABS	PETG	PLA
Birght	ABS	PLA	PETG
Translucent	ABS	PLA	PETG
Hardness	PETG	ABS	PLA
Flexibility	PLA	ABS	PETG
Wrap	PLA	PETG	ABS
Precision	ABS	PETG	PLA
Quality	ABS	PETG	PLA
Chemical resistance	ABS	PLA	PETG
High temperature resistance	PLA	PETG	ABS
Post processing complexity	PLA	PETG	ABS
Machinability	PLA	PETG	ABS
Density	ABS	PLA	PETG
Price	PLA	ABS	PETG

Table 2.5: 3D-printing processes [75].

Process	Advantages	Disadvantages
SLA	Good surface finishing; High layer precision; Opaque and translucent models; Encapsulation models; The printing price of this process has been decreasing.	High cost materials; Support needed; Post processing needed; High printing time comparing to SLS or TDP.
DLP	Printed models can be used for functional tests; Good surface finishing; Cheap process; High materials diversity; Good for screws and threads.	High pre-processing time; high printing time; Support structure needed; Post processing needed.
FDM	Good mechanical model for functional tests: Several materials available (nylon, polycarbonate, etc); Average and high dimensions with good precision; Multi color printing; Low deformation on planar surfaces; Non-toxic materials; No laser needed.	Support structure needed depending on print; High printing time in bigger models; Low surface finishing; Temperature variation during printing process might originate layer separation; Slower process than SLA or SLS; Tight details might lose definition or break easily.
SLS	Several materials available as ceramic composites, nylon, polycarbonate; High autonomy process, low vigilance needed; Fast process comparing to SLA; No need of support; High layer precision; High resistance and life time than SLA models; Recommended for functional models	Parts with porous surface finishing; High cost materials; Nitrogen needed in processing camera for safety during sintering process; Require ventilation and air extraction, so it is not possible to use it in office environment; Several toxic material can be processed.
Solidscape	High quality in obtained models; Good surface finishing: Best process for models with low dimension and high and tight details.	Only wax materials available; High processing time; High post processing time; Support needed; Post processing for support removal.
PolyJet	Elastomer models; Combined materials to guarantee mechanical properties in project specifications; High grey range of printing models; Translucent materials available; Complex geometries; Good finishing surface; Best process for functional threads and screws; Encapsulated models;	Support needed; Post processing need for support removal; Low range of materials available; Low mechanical resistance comparing to SLA; Deformation along time when submitted to radiation
CJP	Do not need support for models; High detail and definition for small dimension models; fast and autonomous process; easy to operate; small machine and easy to transport; cheap process; non toxic materials	low range of materials; the surface finishing is granulated; printed models have low mechanical resistance; dirty post-processing;

Intentionally blank page.

Part II

Prototype Development and Experimental Method

Chapter 3

Prototype development

3.1 Introduction

In the following chapter the development of a conceptual prototype of a bi-functional window blind system is presented.

To start the design of the conceptual prototype it was necessary understand what are the requirements from the functional prototype. The goals are: minimize the light coming from outside when closed; provide privacy from the outside; have a storage system; reduce heat transfers from inside to outside and vice-versa; bi-functional slats to promote and control the heat transfer.

The following chapter was divided in four sections, which are the slat design; the framing; the glazing; and the tilting and lifting mechanisms (figure 3.1). The lifting mechanism was not taken in consideration for the conceptual prototype to simplify, since it would have no impact in thermal analysis experimentation.

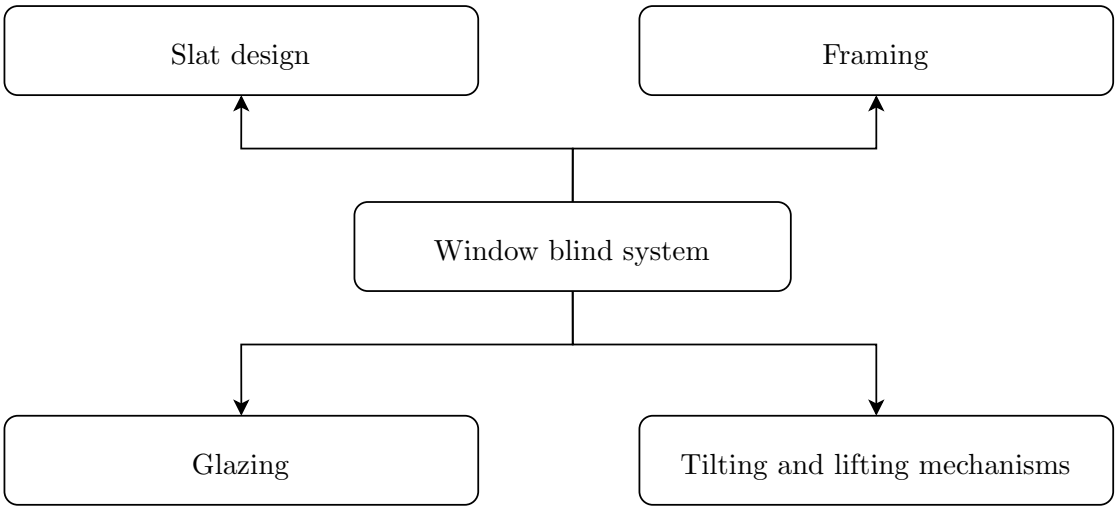

Figure 3.1: Window blind systems

3.2 Slat design

The slat design was focused to maximize the PCM and insulation volumes. Having in mind: the mechanical resistance of the slat should avoid bending and minimize thermal bridges between slats when closed.

To reach the previous goals, the first concept of the slat profiles were drawn (figure 3.2). The slats were splatted into two compartments where they could be filled with PCM and thermal insulator. Simultaneously they could fit each other when the slats are closed and in positions 90°and -90°.

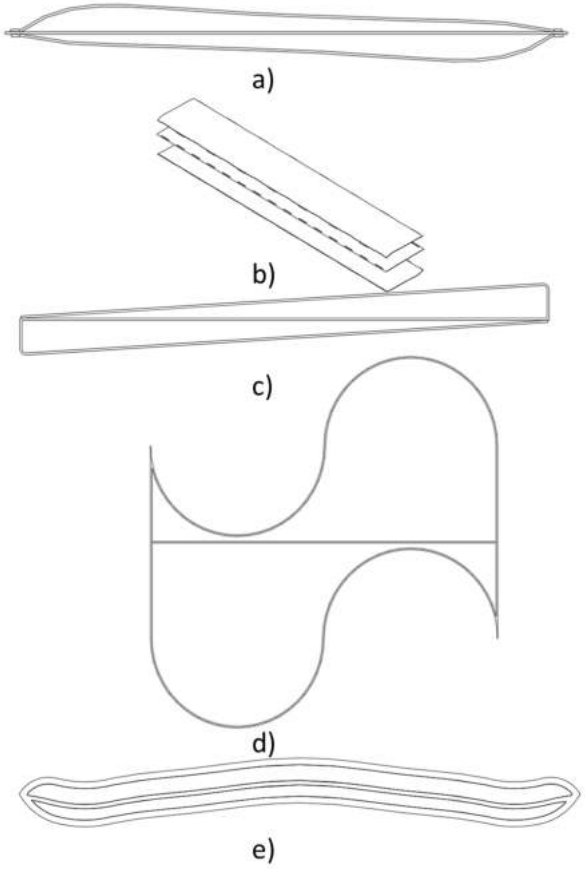

Figure 3.2: First slat profiles (a: design01, b: design01 exploded, c: design02, d: design03, and e: design04

3.2.1 Encapsulation

The encapsulation strategy was the macro capsule in form of a slat. The creation of a robust capsule leads to two main challenges: avoid PCM leakage, which is dependent

on the fabrication method of the slat, and the locking process of the PCM.

The first approach to build the slat was fast prototyping, using FDM process (figure 3.3) due to the easy access and cheap process. As the prototype will deal with temperatures close to 80℃ the chosen material was *PETg* produced by *Tucab* with the specifications presented in table 3.1. The used FDM machine was the Ender 5 produced by *Creality®* and the printing conditions for slat design 6, 6.2 and 7 (presented in subsection 3.2.2) can be found in table 3.2. The selected PCM used for the experimental tests was *Crodatherm 53*, (specifications presented in table 3.3) produced by *Croda®*.

Figure 3.3: FDM printing process of slat and slat holder

Table 3.1: TUCAB PETg specifications [77]

Properties	**Standard**	**Value**	**Unit**
Hardeness	ASTM D785	110	R-scale
Strain stress (50mm/min)	ASTM D638	50	MPa
Rupture stress (50mm/min)	ASTM D638	29	MPa
Elongation (strain) (50mm/min)	ASTM D638	5	%
Elongation (rupture) (50mm/min)	ASTM D638	140	%
Density	ASTM D792	1.27	g/cm^3

Table 3.2: Printing conditions

	Slat design			Units
	6	**6_2**	**7**	
wall thickness	1	1.5	1.5	mm
3D Printer	**CREALITY ENDER 5**			
Noozle diameter	0.4			mm
Printing material	**Tucab - FIL3D PETg (black)**	**Tucab - PETg (transparent)**	**Tucab - PETg (transparent)**	
Slicing software	**ULTIMAKER CURA 4.13.1**			
layer height	0.16	0.28	0.28	mm
infill density	100	100	100	%
printing temperature	245	245	245	℃
build plate temperature	85	85	85	℃
print speed	40	40	40	mm/s

Table 3.3: Crodatherm 53 - specifications [78]

Property	Typical value	Unit
Thermal properties by differential scanning calorimetry (DSC)		
Peak melting temperature	53	℃
Latent heat, melting	226	kJ/kg
Peak crystallisation temperature	51	℃
Latent heat, crystallisation	-225	kJ/kg
Thermal properties by three-layer calorimetry (3LC)		
Peak melting temperature	52	℃
Total heat capacity, melting	220	kJ/kg
Peak crystallisation temperature	52	℃
Total heat capacity, crystallisation	221	kJ/kg
Other properties		
Bio-based content	100	%
Density at 22℃(solid)	904	kg/m^3
Density at 60℃(liquid)	829	kg/m^3
Flash point	250	℃
Specific heat capacity (solid)	1.9	kJ/kg°C
Specific heat capacity (liquid)	2.2	kJ/kg°C
Volume expansion 22℃ – 60℃	9.1	%
Thermal conductivity (solid)	0.28	W/kg°C
Thermal conductivity (liquid)	0.16	W/kg°C
Thermal cycles without change in properties	10000	Cycles

3.2.2 Slat filling tests

The slat design 06 (figure 3.4), was used for the first test. This design is composed by a 1 mm thickness wall slat, with 290 mm length. It was splatted in two compartments to

fill with insulation material and PCM. Two holes were designed for the lifting mechanism. In the PCM side a hole for filling and a level plug hole, were designed. The bottom of the slat is closed as seen in figure 3.4. The used oven for the filling experimentation was produced by *Heraeus* and it was equipped with an *Eurotherm 3216* temperature controller.

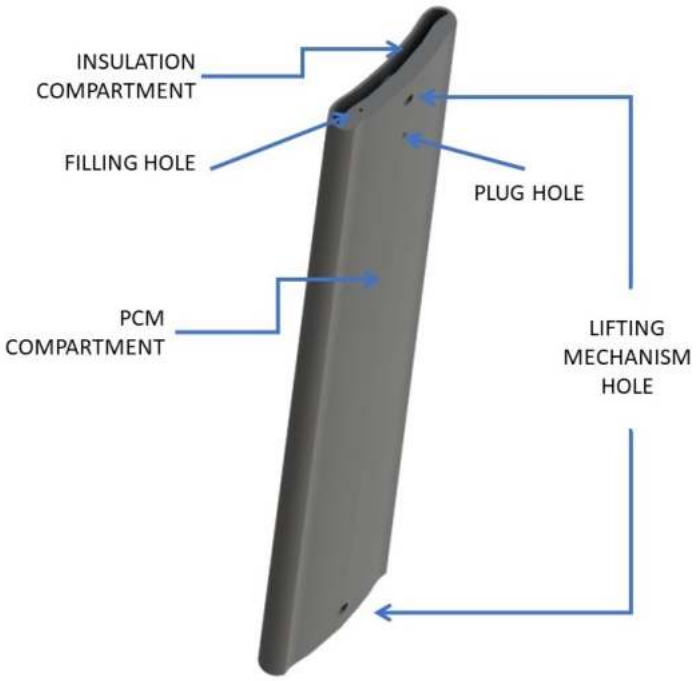

Figure 3.4: Slat design 06 schematics

The followed procedure was done for the experimental test:

- PCM was left inside the oven under 60℃ for 24 hours in order to get fully melted;
- The slat was held by printed support (figure 3.3);
- A 5ml syringe was used to insert the PCM inside the slat (figure 3.5a);
- Wait until the PCM reaches rooms temperature;
- Open the slat to check if the PCM reached all the volume.

After the **first experimental test** several difficulties were found: the filling hole was opened with a drill after the first try; the syringe was clogging when moving the PCM due to phase change; level hole to keep PCM volume under the limit did not work also because of phase change; the dark colour of the printed slat did not allow to check the level of PCM quantity inside, which forced to cut it in half (figure 3.5b).

(a) Experimental process (b) Result (slat cut in half)

Figure 3.5: First experimental test (slat design 06)

In the **second experimental test** several upgrades were made: transparent filament was used to verify the level of PCM inside the slat; the slat design 06 was redesigned, the wall thickness was raised to 1.5 mm, the filling hole diameter was raised to 3 mm; and the level plug which did not worked was replaced by a printed groove.

It was also created design 07 (figure 3.6). considering improvements of the continuity in insulation layer.

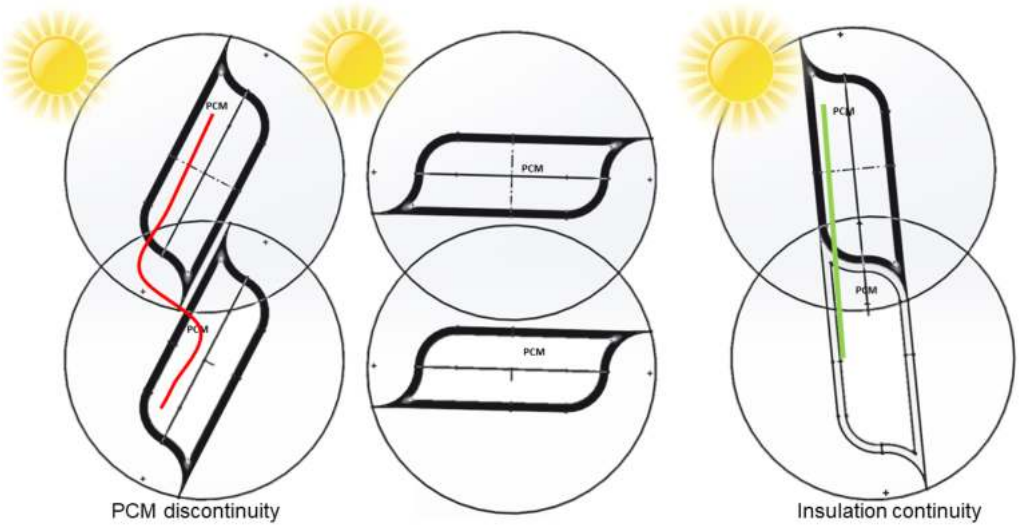

Figure 3.6: Slat design 07 profile - concept principles

The two designs (design 06V2 and design 07) were tested (figure 3.7). Since the used filament when printed is translucent, a dye was added when filling design 06v2 to make easier the filling procedure.

Using the same 5ml syringe, the process was replicated, not allowing the oven to decrease under 53℃. This time slats were left inside the oven to let the PCM melt and homogeneously.

After filling the slats, they were both left in the oven for 24 hours (figure 3.7a), to check if there were any leakages. The slats were cut in half to verify if there was any PCM left and where is was placed.

As seen in figure 3.7b both slats were almost empty, although some PCM was still at the bottom. Which provided the doubt if there was a deformation in the slat due to oven temperatures oscillation.

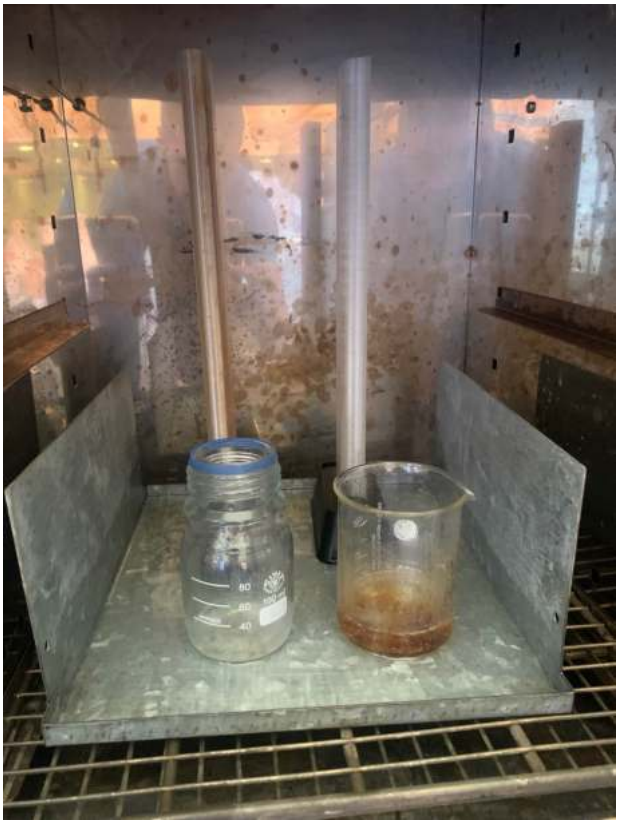

(a) 2nd experimental process

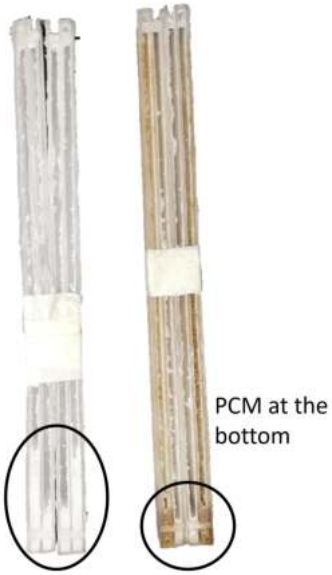

(b) Experimental results

Figure 3.7: Second experimentation (slat design 06v2 in brown and slat design 07 in white)

3.2.3 PCM leaking through FDM process experimentation's

To clarify the leak tightness of the slat, 5 cups were fabricated. The cups dimensions were $25 \times 25 \times 30mm$. The different printing conditions used are presented in table 3.4.

Table 3.4: Printing conditions - Leakage experimental test

Designation	**Dimensions**(mm^3)	**Wall thickness**(mm)	**Layer height**(mm)
1	25x25x30	0.5	0.28
2	25x25x30	1.5	0.12
3	25x25x30	1.5	0.28
4	25x25x30	2	0.12
5	25x25x30	2	0.28

The cups were left inside the oven for 4 days (figure 3.8a), and the temperature was monitored with *testo 175-T3* temperature logger (figure 3.8b), to understand if the inside temperature was constant. The software *Testo - ComSoft Basic* was used to export the values and analyze them. As shown in figure 3.9 the inside temperature of the oven was constant on the 58℃ during all the experimental test.

(a) Proving cups inside the oven

(b) Testo 175-T3 [79]

Figure 3.8: Experimental process

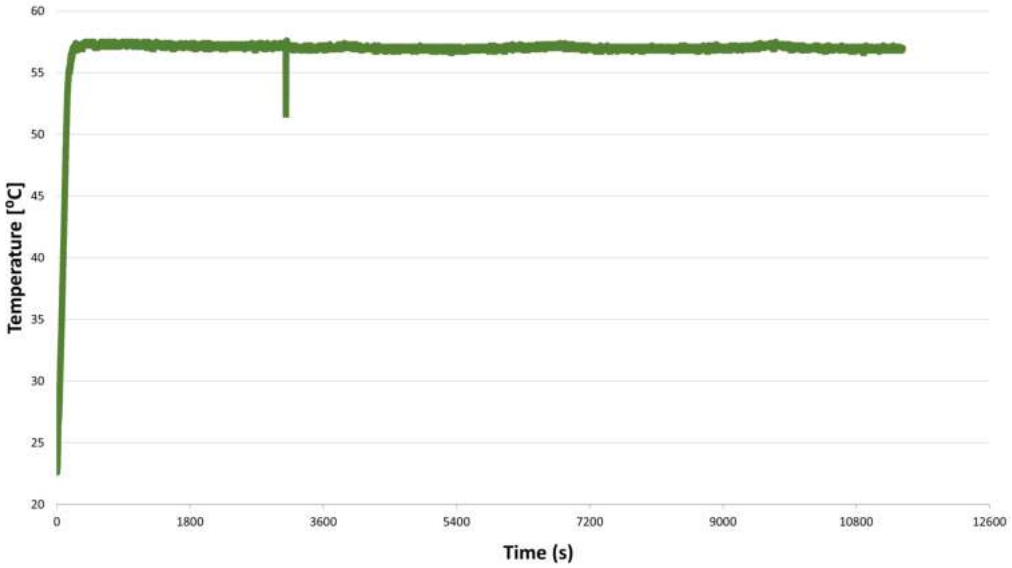

Figure 3.9: Temperature log inside of oven

It is possible to conclude that was no deformation on the printed part caused by temperature rise. Analysing figure 3.10 it is stated there were leaks through all the cups. The cups were all filled to the top (when the PCM was in solid state), and the black lines marked in the cups in figure 3.10 show the PCM level after the experimental test. It is possible to decrease the leakage by increasing the wall thickness and the layer thickness of the printed part. Since the wall thickness of the printed slat must match a close value to the standard slats and it is needed a solution with zero leaks, the FDM process was shown not be viable for this specific application and experimental test.

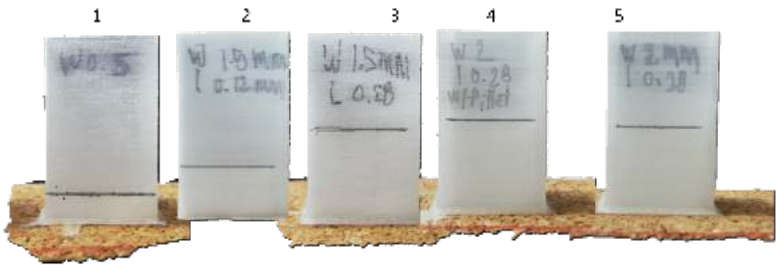

Figure 3.10: Experimentation results -Leakage experimental test

3.2.4 Aluminium slats

Since no viable solution through FDM fabrication process was found, the investigation proceeded with commercialized aluminium slats.The conceptual prototype uses two different aluminium slats. In figure 3.11a it is presented the convectional aluminium slat filled with polyurethane foam with a wall thickness of 0.5 mm. In figure 3.11b it is presented other aluminium slat, with a wall thickness of 1.1 mm, which was filled with the PCM. The slat length was 230 mm.

(a) Slat with polyurethane foam (b) Slat with PCM

Figure 3.11: Aluminium slats profiles

The PCM filling process was similar to subsection 3.2.2. When the PCM was in solid state, the weight was measured in all slats to guarantee the fulfil of PCM (table 3.5). The average mass of the slat filled with PCM is 69.28g which can be concluded that the average PCM quantity in each slat is 16.08g.

Table 3.5: Slats weight

Slat number	**mass (g)**
slat 1	70.2
slat 2	70.2
slat 3	69.6
slat 4	68.8
slat 5	68.6
slat 6	68.3
$\overline{m}$	69.28
empty slat	53.2

To seal the slats on both extremities, after being degreased, a high temperature silicone (*Silkron SPG* from the company *Krafft®*) was used.

3.3 Framing

To develop the frame for the conceptual prototype the FDM fast prototyping process was used. The frame (figure 3.12) is composed by four main parts which are modular and assembly in each other. Three of the parts are equal, the fourth which is placed in the top of the prototype (figure 3.13) has two holes to fit two thermal sensors for the experimental tests.

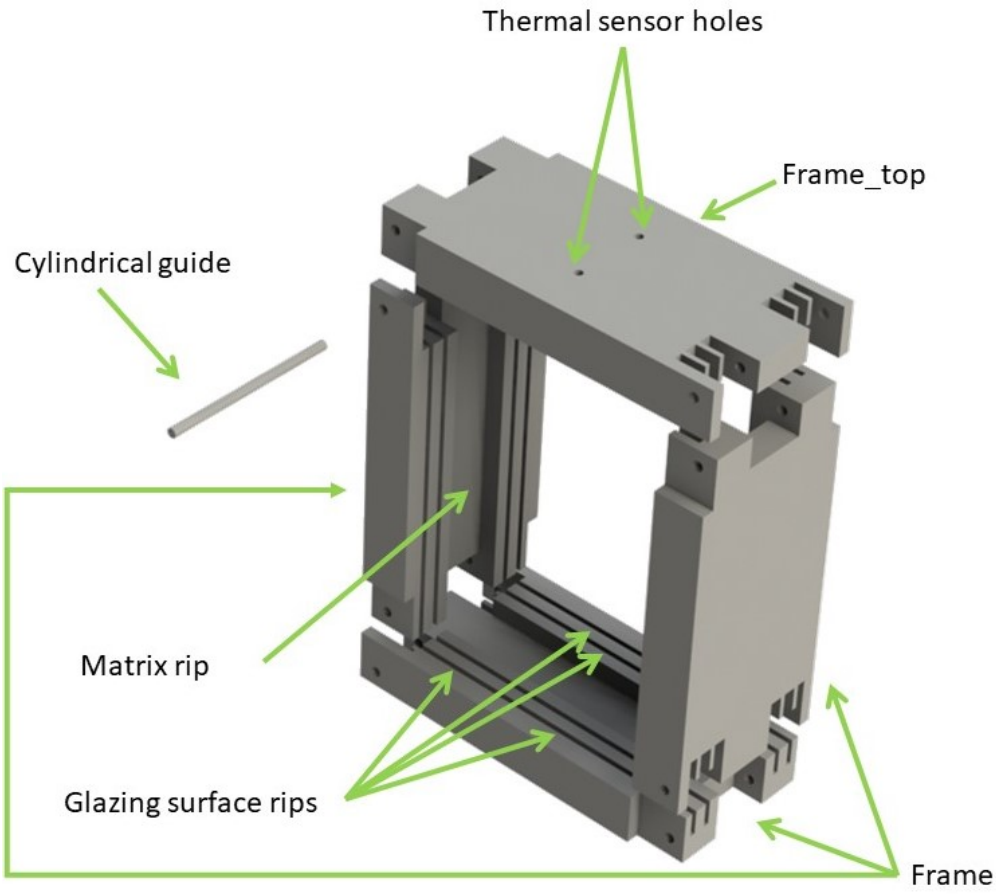

Figure 3.12: Framing assembly - exploded view

Figure 3.13: Top frame - printed part

The framing dimensions are dependent on the printable volume of the 3D printing machine, which is limited to 300 mm on the Z axis. The assembled frame parts define the prototype volume, which is $290 \times 290 \times 140$ mm^3. The framing section is composed by five rips: four to fit the glazing surfaces, and in the middle to fit the matrix for the slats orientation, as seen in the definition draws in appendix A (figures A.2 and A.6). The four parts are held by a cylindrical guide with 7.5 mm diameter and length of 140 mm, also produced with FDM process (appendix A (figure A.5)). The printing conditions from the prototype parts can be found in the table 3.6.

Table 3.6: Printing parameters - prototype

Part name	**frame**	**frame_top**	**cylindrical guide**	**slat matrixes**	**Units**
3D Printer	CREALITY ENDER 5				
Noozle diameter	0.4				mm
Printing material	Tucab - FIL3D PETg (black)				
Slicing software	ULTIMAKER CURA 4.13.1				
layer height	0.28				mm
infill density	30				%
printing temperature	245				℃
build plate temperature	85				℃
print speed	40				$\mathrm{mm\,s^{-1}}$
printing time	45	45	1.5	15	h

3.3.1 Glazing surfaces

The glazing surfaces are fixed by the framing (figure 3.14), and are composed by four glasses of 248×248 mm^2 with 4 mm thickness. The four glasses represent a conventional double glazing system. The glass properties can be found in table 3.7 and the glass technical draw is presented in appendix A (figure A.3).

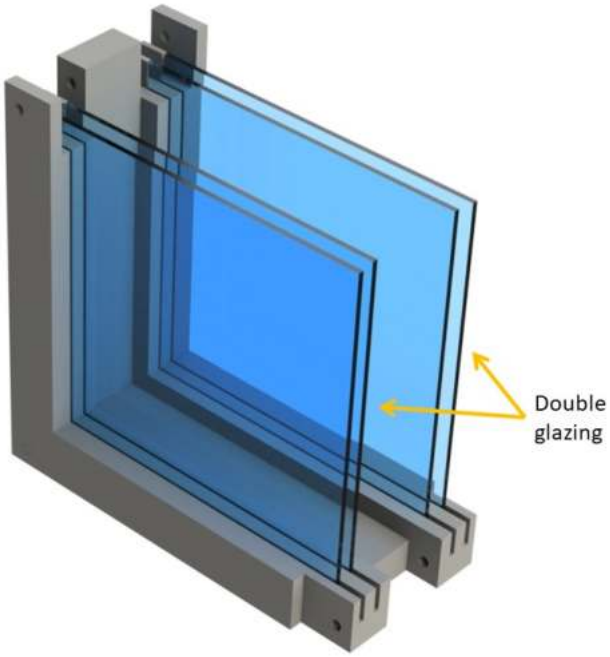

Figure 3.14: Glazing surfaces

Table 3.7: Glass properties [80]

Properties	Value	Unit
Thickness	4	mm
Density	2500	$kg\,m^{-3}$
Thermal conductivity	1	W/m°C

3.4 Tilting positioning

The tilting mechanism was developed with three different matrices that fit in the lateral frame parts.

The matrices guarantee different positions of the slats (figure 3.15): slats in 90° position - fully closed (figure 3.16a), slats with 0°, fully opened (figure 3.16b). It was also developed the project of slats in 45° which was not furtherly tested. The matrices technical draws can be found in appendix A in figures A.4,A.7 and A.8.

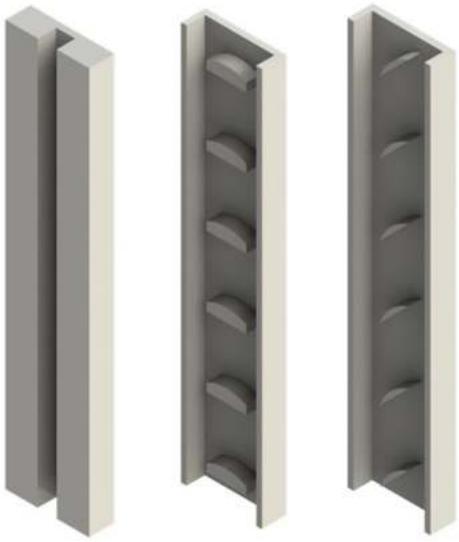

Figure 3.15: Matrices render image (from left to right): 90° slat; 0° slat; 45° slat

(a) Closed position (b) Open position

Figure 3.16: Closed and open matrices with slats

The slats are held by the matrices. As shown in figure 3.17 to change the inclination of the slat, it is needed to disassembly the top part of the frame, and replace by the selected matrix .

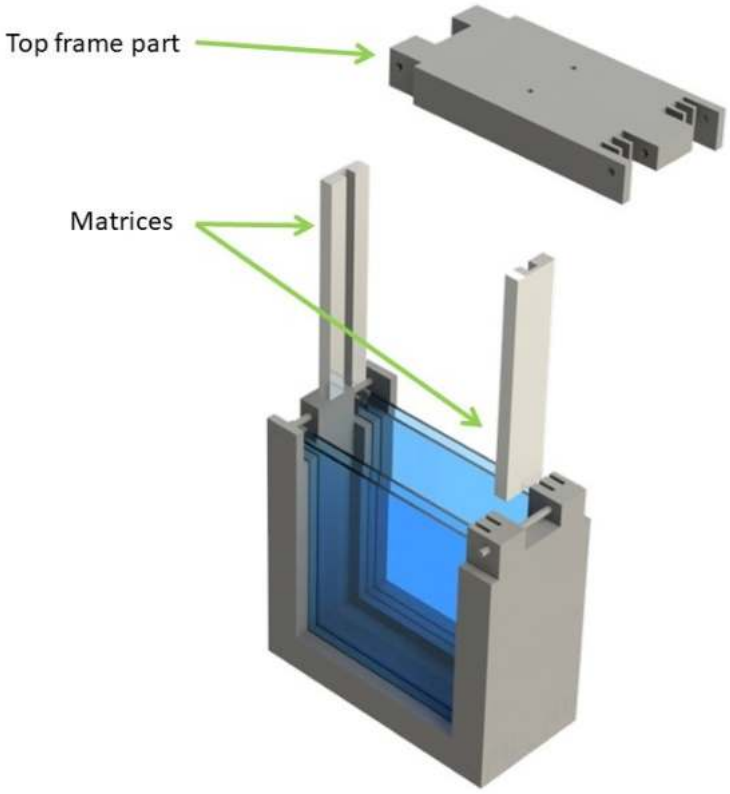

Figure 3.17: Matrix replacement

3.5 Prototype assembly

The full concept prototype do not request any tool to be assembled. The assembly sequence start with the assembly of the side frame parts to the bottom part using two cylindrical guides. Later, the four glasses can be fitted from the top. After, the slats can be fitted with the tilting matrix. The last step is to fit the top frame and insert the two cylindrical guides.

Figures 3.18a and 3.18b, presents the final prototype fully assembled, with two different slat matrix - opened (figure 3.18a) and closed (figure 3.18b). It is possible to check the assembly technical draw of the prototype in appendix A (figure A.1).

(a) Prototype with open slat matrix

(b) Prototype with closed slat matrix

Figure 3.18: Prototype with open and closed slat positions

Chapter 4

Experimental process and results

4.1 Introduction

The following chapter is composed by three sections. The experimental process presents the procedure and the work sequence in the laboratory. The experimental results present the experimental tests and results analysis. The limitations and possible upgrades are presented in the last section.

4.2 Experimental process

The experimental test was carried out in the Smart Plastic Lab in the Mechanical Engineering Department of *Universidade de Aveiro*. The required materials and equipment were the oven *Heraeus®* equipped with an *Eurotherm® 3216* temperature controller, also used in subsection 3.2.2; the bi-functional blind system conceptual prototype; the instrumentation devices, and a thermographical camera (*Fluke® - Ti S20*) .

4.2.1 Instrumentation

In order to analyse and evaluate the thermal performance of the PCM, it was used temperature sensors.

In the top framing two holes with 6.5 *mm* diameter were designed to insert two PT100 thermal sensors (figure 4.1a). The PT100 are RTD (Resistance Temperature Detector) which associate a temperature to a resistance. The PT100 sensors have an associated error of ±0.01℃. *MAX31865* (figure 4.1b) boards were used to convert measured resistance of the sensor into temperature and send it to the microcontroller, using the SPI (Serial Peripheral Interface) communication protocol. The used microcontroller was the *ESP8266 Nodemcu V3* (figure 4.1c). The controller was programmed using C++ language, to read the temperatures and send them directly to *Google sheets* ((figure 4.1d) using *Wi-fi* connection. The *Google sheets* spreadsheet was chosen due to an easy interface with the user, and it was added a chart to see the measured values. In a first approach, the microcontroller was sending the measured values each 5 minutes. In

later experimental tests, the controller was programmed to send data each 1 minute to avoid data noise. The instrumentation schematics is presented in figure 4.1. In figure B.1 (appendix B) is presented an image from the used instrumentation, with a *smartphone* used as hotspot for the ESP8266 to connect to *Wi-fi*

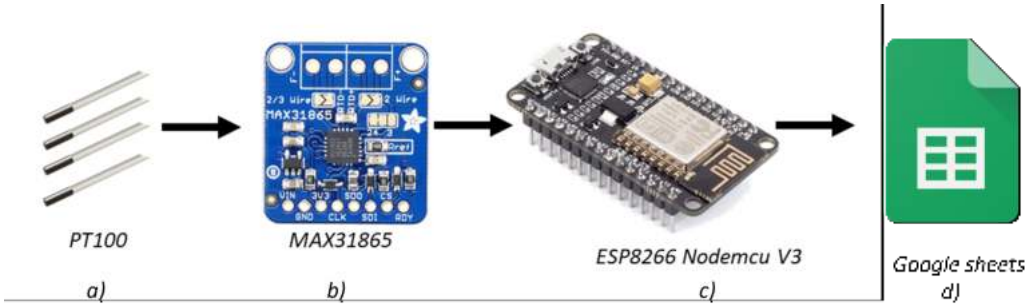

Figure 4.1: Instrumentation of data acquisition

4.2.2 Laboratory apparatus

The experimental scheme is presented in Figure 4.2. The oven represents the outside conditions and it is settled to a temperature that can melt the PCM. The oven is composed by three resistances (located at the bottom and side walls) and a fan (located at the back wall). The PT100 thermal sensors will be placed as shown in schematics (figure 4.2): glass surface temperature (T1), after the slats (T2), before the slats (T3), and inside the oven (T4).

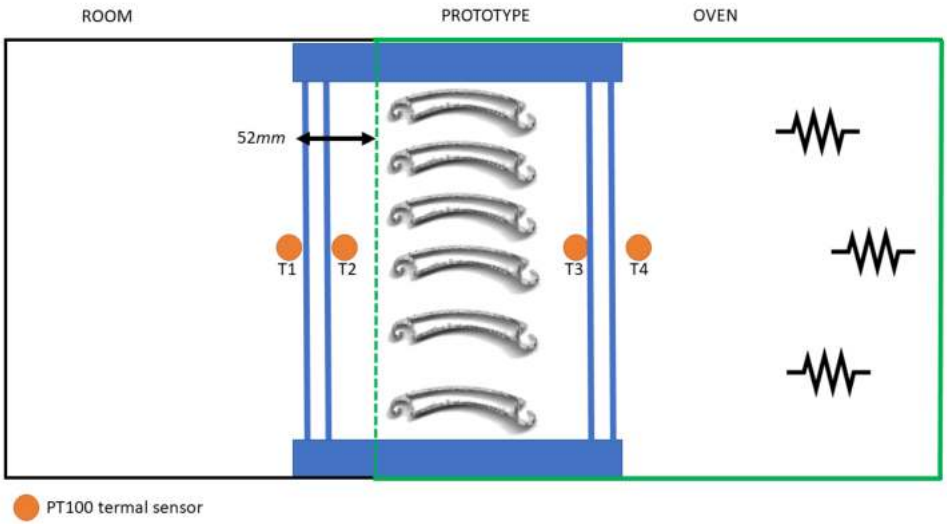

Figure 4.2: Experimentation - schematics

As seen in figure 4.3, the prototype is held to the oven by two tight XPS (extruded polystyrene insulation) plates with 40 *mm* thickness, preventing the heat losses around the prototype. The thermographic camera it is used to check where the heat flux goes, and to identify possible the thermal bridges.

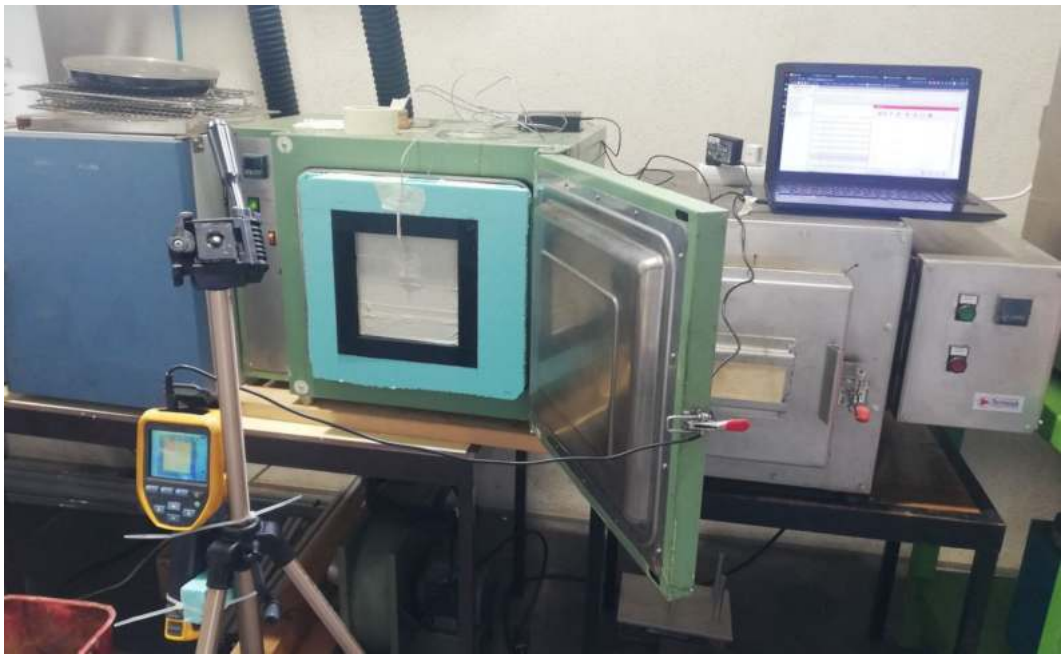

Figure 4.3: Experimental apparatus

4.2.3 Laboratory procedure

The laboratory procedure is repeated for four different setups. Two different slat positions (0° and 90°) were tested with slats filled with polyurethane foam and slats filled with PCM. The following steps were taken:

1. Assembly the prototype using the selected slat type;
2. Hold the prototype in the oven's door (figure 4.2);
3. Start temperature measurements;
4. Warm up the oven until 65℃;
5. Monitoring the temperatures using ESP2866 with a time interval of 1 minute;
6. Take thermal images using *Fluke®* - *Ti S20* with a time interval of 10 minutes;
7. Turn off oven resistances;

8. Stop measurements;

9. Repeat sequence with different slats and different position.

4.3 Experimental results

The experimental tests were made to evaluate the PCM performance only in the charging phase. Small voltage oscillation in the microcontroller influence the measured temperature values, which implies noise in exported data. The noise was reduced using Moving Average filter in *Excel*, that uses equation 4.1, with an N = 6.

$$F_{l+1} = \frac{1}{N} \sum_{j=1}^{N} A_{l-j+1} \tag{4.1}$$

Where:

- N is the number of prior periods to include in the moving average;
- A_j is the actual value at time j;
- F_j is the forecasted value at time j.

It is important to mention that after the experimental test with the slats filled with PCM, the slats weight had a difference of $\Delta m = \mp 0.3\%$, from the previous measurements with an average slat weight of $\overline{m} = 69.28g$ (table 3.5), due to device error .

4.3.1 Open slats

Observing the temperature profiles with the open slats matrix in figure 4.5, it is possible to see that the temperature profiles in the PCM slat and in the convectional slat are very similar. Considering the measurement after 0.75 hours to 3.25 hours presented in figure 4.6, it was calculated the temperature difference. The average difference for profiles T2 and T2 (PCM) in this interval was 0.97℃, and for profiles T3 and T3 (PCM) was 0.18℃.

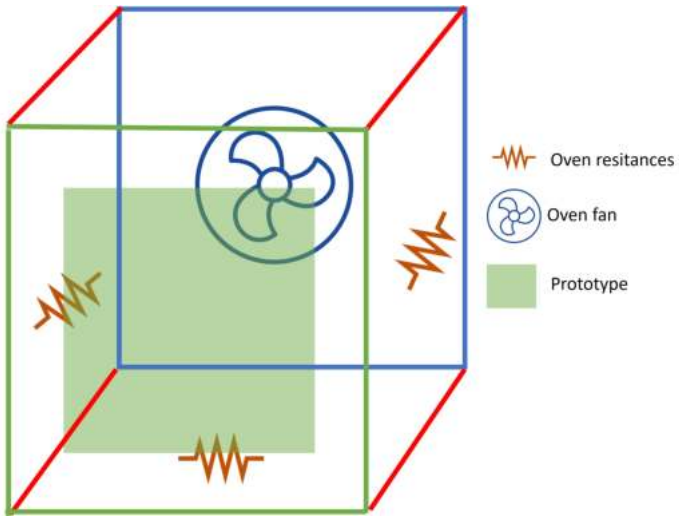

Figure 4.4: Oven scheme

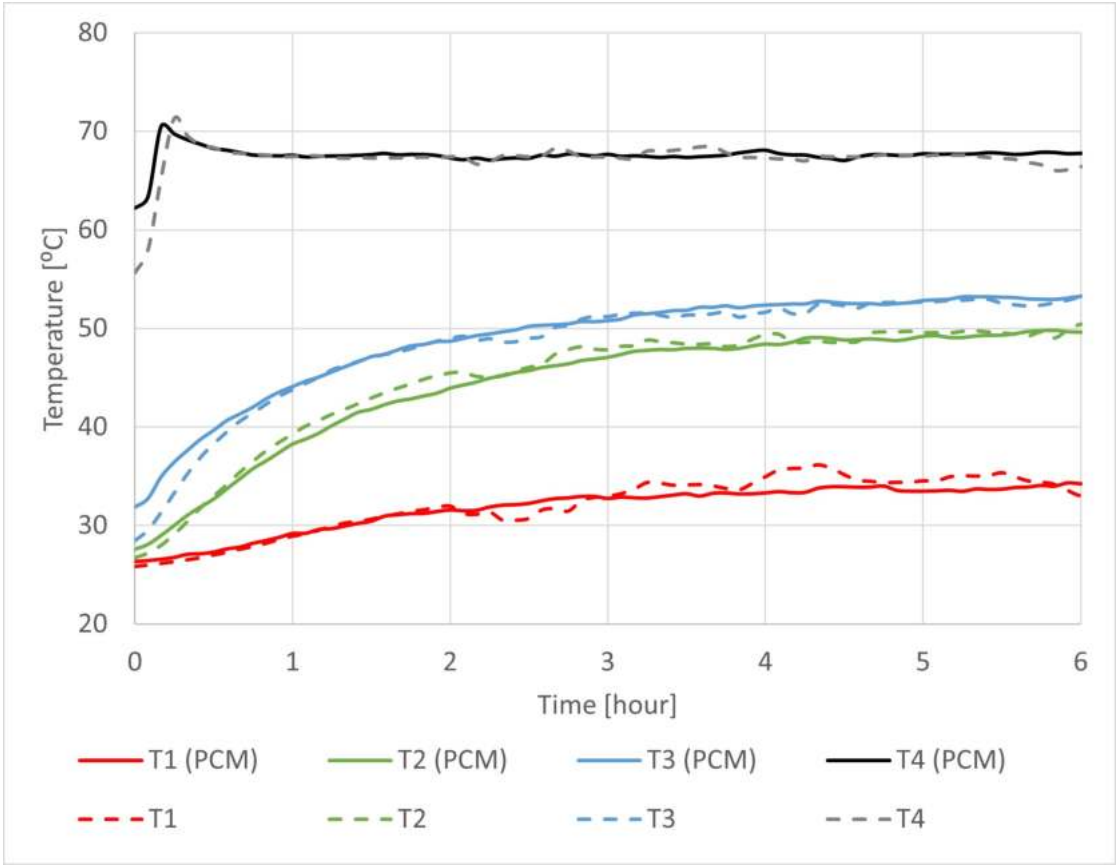

Figure 4.5: Open slats experimental test - temperature

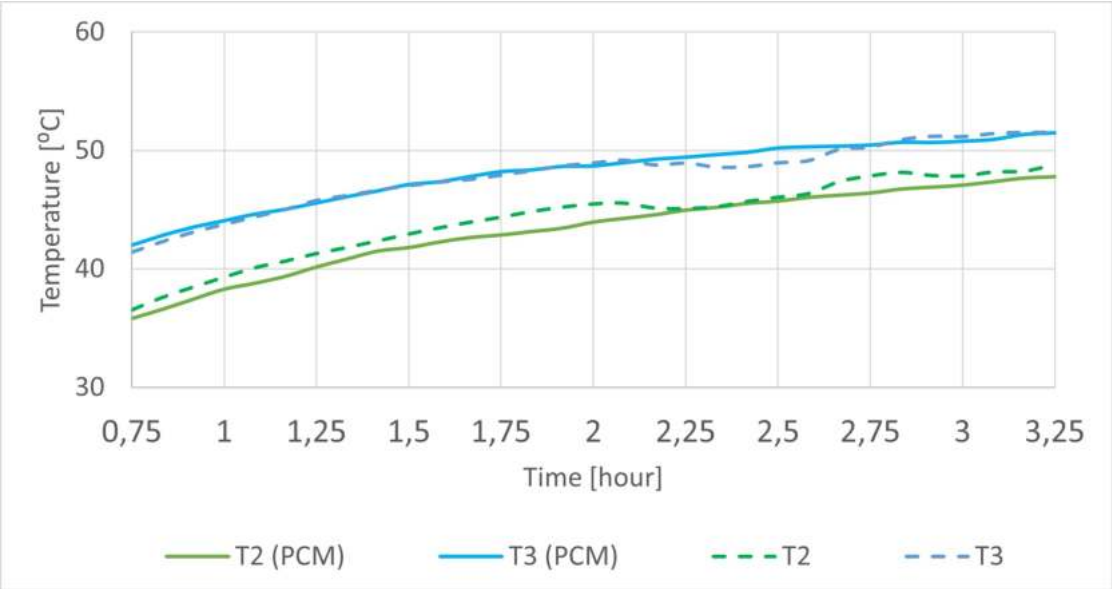

Figure 4.6: Open slats experimental test - temperature from 0.75 hour to 3.25 for T2 and T3

The thermal image from the experimental test with open slats is shown in figure 4.7. In figure 4.7a, the temperature of the prototype and surroundings was almost homogeneous with only 2℃ of difference. In figure 4.7b the temperature difference was 11℃ and it is evident that the heat flux went towards the top of the prototype which is explained by the position of the oven resistances (two on the sides and one at the bottom) and the fan in the back (figure 4.4). When the air temperature raises, as other materials, it increase its volume, which create more space between molecules and, as consequence, the air remains with less density and float to the top of the prototype.

In figure 4.8, initial and final conditions from the experimental test with open slats with PCM are shown. The beginning of the experimental test (figure 4.8a), the temperature difference was 3℃ and the warmest part was the left. This happened because the oven was next to another oven which was turned on. The end of the experimental test (figure 4.8b) the temperature difference was 10℃ and the warmest part still the top of the glass due to aforementioned explanation.

When comparing PCM slats with conventional slats in window blinds systems, when they are settled in open positions (0°) there are no thermal disadvantages found. In the other and, all the goals from a convectional slat can be acquired with the PCM slats as natural light, viewing factor.

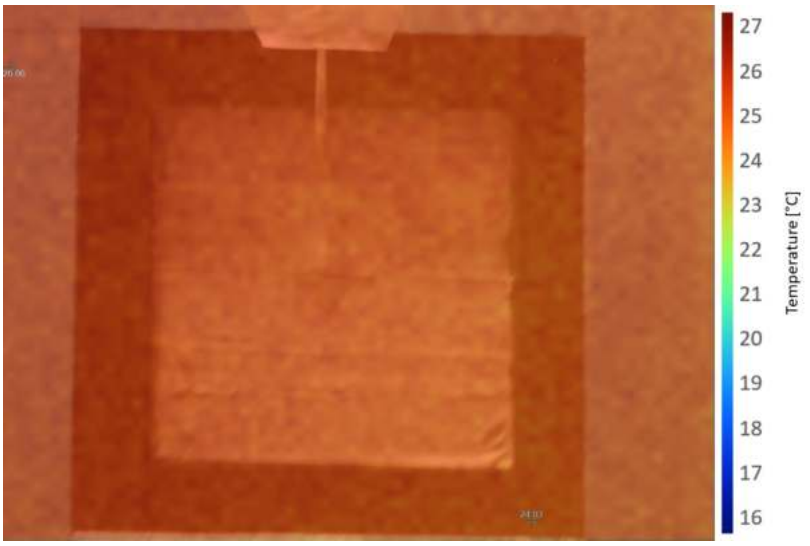

(a) Beginning of experimental test

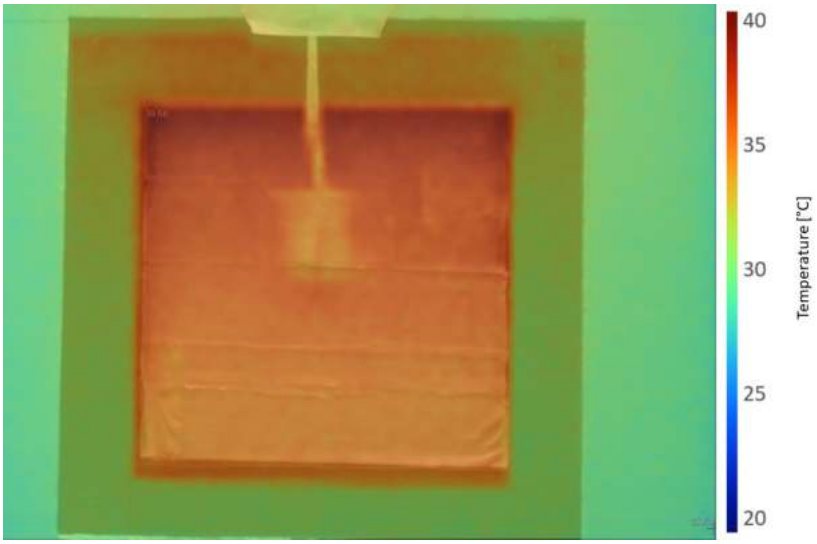

(b) End of experimental test

Figure 4.7: Open conventional slats - thermographic camera

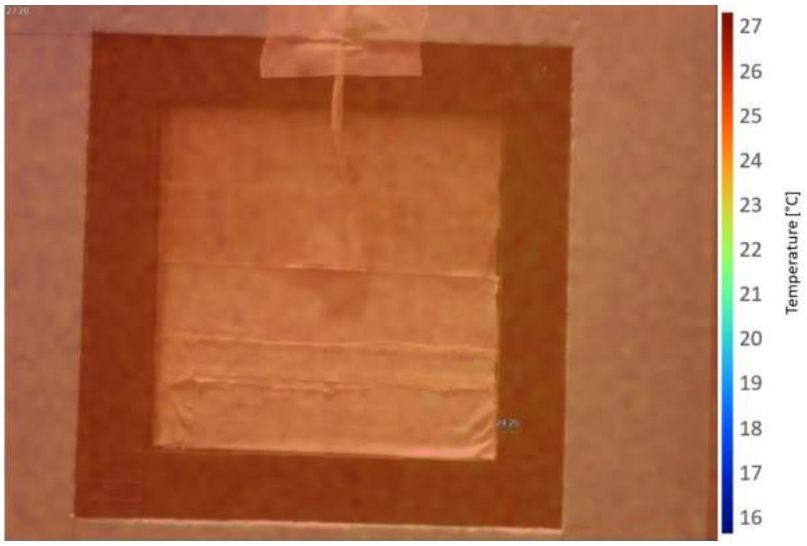

(a) Beginning of experimental test

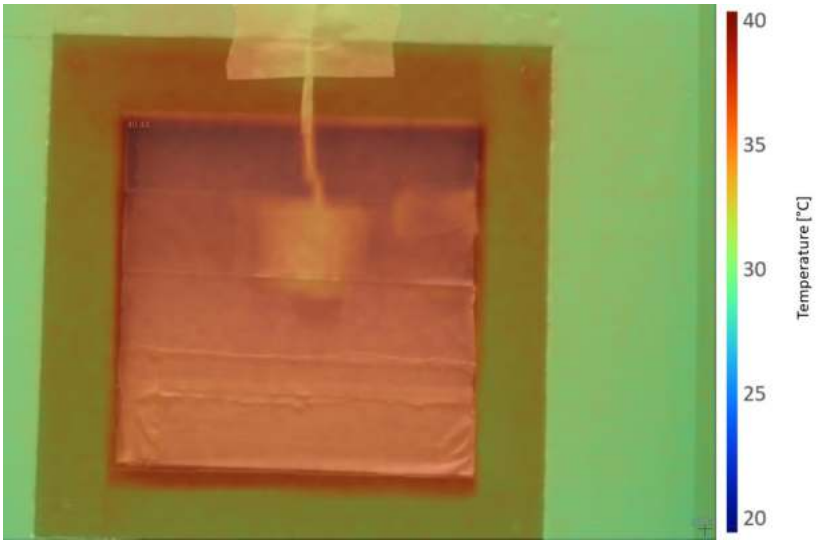

(b) End of experimental test

Figure 4.8: Open slats with PCM - thermographic camera

4.3.2 Closed slats - experimental test 1

Observing the temperature results with the closed slats matrix (figure 4.9), it is possible to see that the temperature profiles in the PCM slats and in the convectional slats are similar. With this experimental test with closed slats, it was stated that the temperature sensor after the slats (T2 - PCM) never reached the PCM melting temperature (53℃) presented by the manufacturer. Therefore, it is possible the temperature inside slat is higher than the measured in T2 (47℃) due to air resistance through convection. Being

the inside slat temperature (51℃) value far from the pretended (53℃). Due to this inconclusive measures, new experimental tests were done. In addition, the thermographic camera data is presented in appendix C in figs. C.1a, C.1b, C.2a and C.2b.

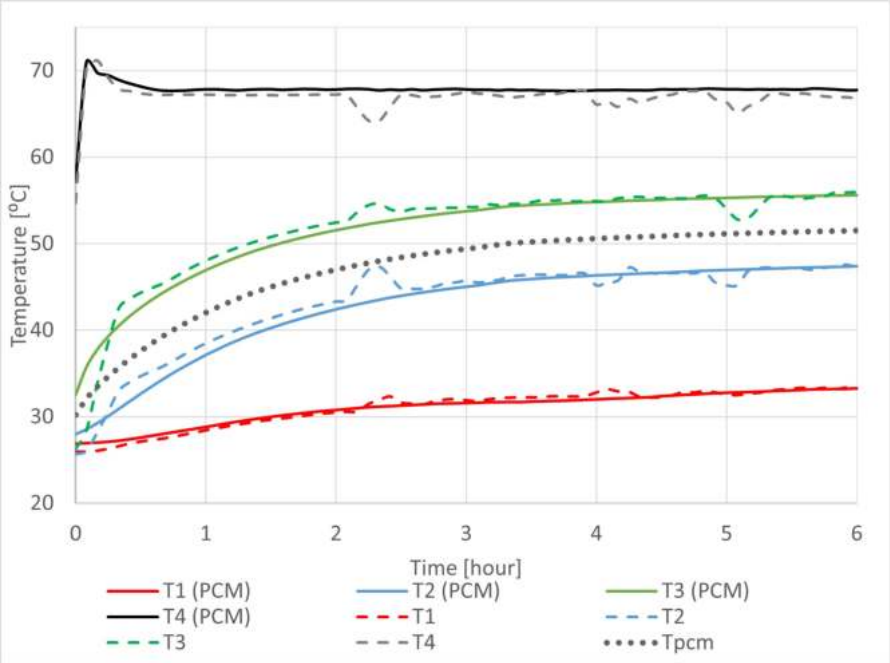

Figure 4.9: Closed slats experimental test 1 - temperature

4.3.3 Closed slats - experimental test 2

In this new experimental tests, a few corrections were done: the oven temperature was raised to 76℃; the PT100 measuring T2 and T3 were stacked on the slat surfaces (figure B.2 from appendix B). Due to PCM leaking no thermal sensor was added inside the slat, so the PCM temperature was calculated by the average of T2 and T3. The thermographic camera data for the experimental test with closed slats 2 is presented in appendix C, in figures C.4 and C.3. The heat flux has evolved as predicted and explained in subsection 4.3.1.

In figure 4.10, the temperatures results are presented. The first maximum on T4 and T4 PCM is due to the oven temperature stabilization. The second maximum relative in T4 PCM is due to a manual temperature rise, of 3℃, from the oven to guarantee the inside slat temperature to reach PCM melting temperature defined by the manufacturer. By the end of the experimental test (6 hours) the PCM reached 53℃, so it still was in the phase change process. Considering the objective is to melt the PCM completely, longer experimental test should have been done, or higher heat exchange rate should be set.

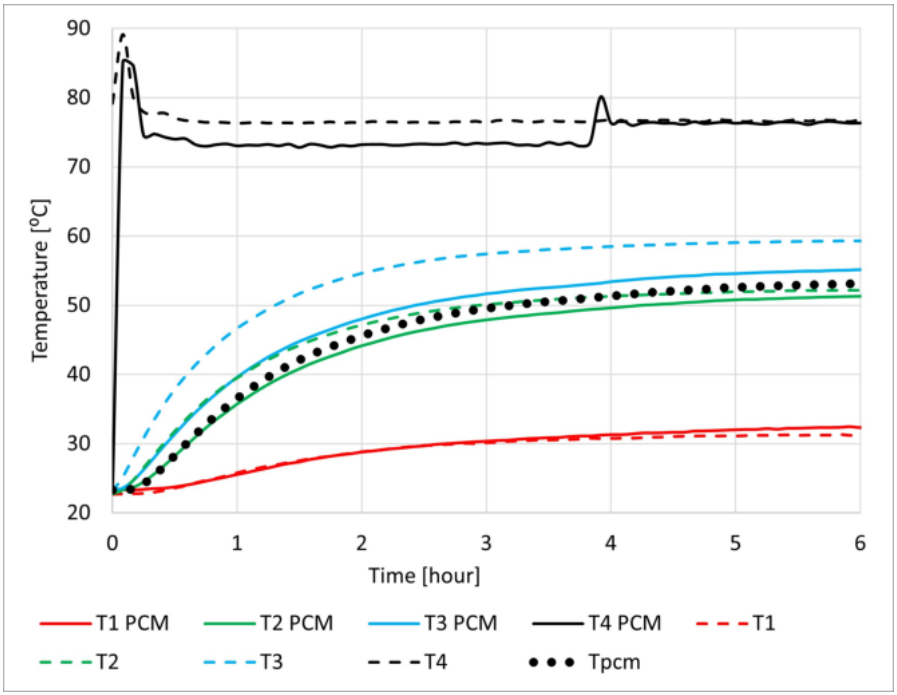

Figure 4.10: Closed slats experimental test 2 - temperature

4.3.4 Closed slats - experimental test 3

With the conclusions taken from previous experimental test, a third experimental test was done following the same procedure as the second was carried out but with a temperature set to 86℃. This was the temperature limit for PETg to not suffer deformation. The thermographic camera data for the experimental test with closed slats 3 is presented in appendix C, in figures C.6 and C.5.

The presented PCM effect range in figure 4.11, is from PCM temperature 51.15℃ to 57.5℃. It is possible to see the temperatures T3 PCM and T2 PCM standing with slope of almost 0°, this happens during PCM effect because the phase change is an endothermic reaction. Analysing the beginning of the PCM effect phase, the temperature difference between T3 PCM and T2 PCM is 8.69℃, with a PCM temperature of 51.16℃ and it decreases to 7.89℃ by the end of the phase change effect with a PCM temperature of 57.5℃. This happened because after the latent phase, the slat tend to reach the equilibrium temperature which will converge in a constant temperature. By the end of the experimental test the temperature difference was lower (6.6℃), and tend to get closer because the slope of T2 PCM is higher than the slope of T3 PCM.

In the convectional slats, the temperature differences between the the T3 and T2, in the three analysed stages were almost constant with a difference of 5.97℃, 6.05℃ and 6.09℃. This happened because the convectional slats were not submitted to a phase change reaction neither a latent phase.

The temperature difference between T3 PCM and T3 was 0.55℃ and between T2

PCM and T2 was 1.56℃ in the beginning of the PCM effect phase and decreased to -2.02℃ and to -3.86℃ respectively. This happened because the convectional slats temperature kept reaching the equilibrium temperature, while the slats with PCM where in the charging phase, using the transferred energy to change its phase. It is important to notice that the highest temperature difference, during phase change effect,between T3 PCM and T3 was 2.09℃ and between T2 PCM and T2 was 4.1℃.

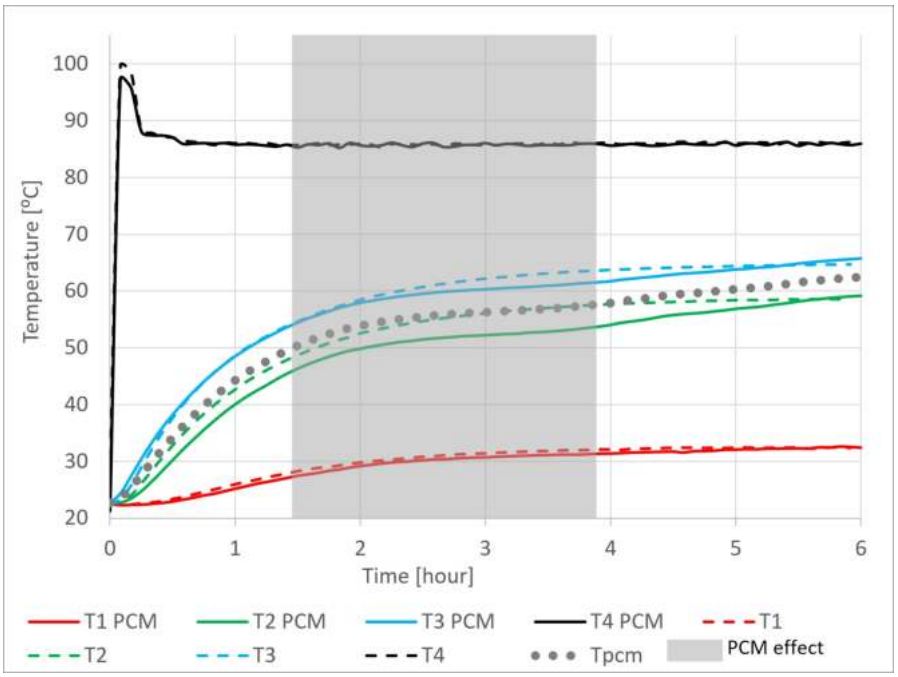

Figure 4.11: Closed slats experimental test 3 - temperature

Analysing the inside slat temperatures, a comparison between the temperature of the slats with PCM and the convectional was done. The slats temperature was considered as the average between T2 and T3. In figure 4.12 it is understandable that in the first hour of the experimental test the temperature from the slat with PCM was above the conventional slat, reaching a temperature difference peak of +11%. This happened because the thermal conductivity from PCM is 7 times higher than the PU foam (table 4.1). After the first hour, the PCM started to enter in the latent phase and its temperature started to increase slower, as previously presented, becoming under the convectional slat temperature for 4.5 hours and during this period it reached a temperature difference of -5.13%. Although the PCM conductivity being higher than the PU foam it took 5.5 hours for the PCM to reach the conventional slat equilibrium temperature.

In real application, the window blind system with PCM will be submitted to heat transfer mainly by radiation, and its temperature profile will not be always rising. From previous conclusions it is noticeable that peak temperature can be retarded when using slats filled with PCM.

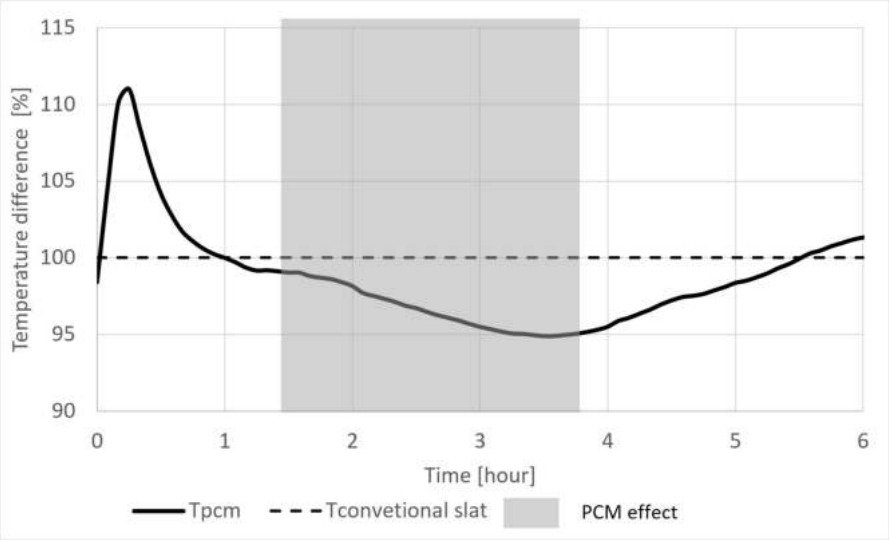

Figure 4.12: Slats temperature difference

Table 4.1: Materials properties (300K)

	Value	**Units**
k_{glass} [80]	1	W/mK
L_{glass}	0.004	m
A	0.0441	m^2
h_{air} [81]	12	W/m^2K
k_{al} [81]	237	W/mK
$L_{al,PUfoam}$	0.0005	m
$L_{al,pcm}$	0.0011	m
k_{PUfoam} [80]	0.04	W/mK
L_{PUfoam}	0.00335	m
$k_{pcm,solid}$ [78]	0.28	W/mK
L_{pcm}	0.0028	m

4.4 Work limitations

During the experimental tests several limitations were found in the prototype, instrumentation, and laboratory procedure.

The first approach for temperature log was to connect the ESP8266 to another online database. This approach was not robust, the ESP2866 connection to the data base was not always working. Later, a new program was developed and the data log started to be directly on the computer, which implies the connection between the ESP8266 and the

computer. Finally, the last program which communicates with *Google sheet* database was robust and trustable.

Furthermore, when treating the data log in the worksheet it was noticed a lot of noise in the measurements. To minimize the noise, the moving average filter from the *excel* was applied. Later, the program was changed to send data each 1 minute, and in the spreadsheet the data from each 5 measurements was selected. This resulted in an almost clean data values.

Another limitation found was that the thermographic camera was not able to measure the temperature directly in the glass surface, which was solved with paper tape avoiding the reflection.

The prototype itself is limited because it is not possible to change the tilting angle from the slats with the prototype closed, as a result, it is only possible to do experimental tests to each tilt angle at a time. Another limitation is the material deformation temperature, which rounds the 85℃. Hence, for applications that need higher temperatures another material for the prototype should be chosen.

4.5 Future work

In the future the prototype can be upgraded changing the top frame and adding the tilting mechanism as a response to the limitation found in section 4.4, which will allow the user to define heat releasing direction according with the thermal necessities.

The presented solution for the tilting mechanism (figure 4.13) only requires a new top frame part, due to two new slots presented in figure 4.14a. The suggested mechanism is composed by a stepper motor, which can be programmed for the pretended slats inclination. The stepper is connected to a transmission shaft, held by the mechanism support which has coupled axial bearings (figure 4.14a). On each side of the transmission shaft a spur gear is placed to drive the slats simultaneously with a toothed belt (figure 4.14b).

Figure 4.13: Tilting mechanism

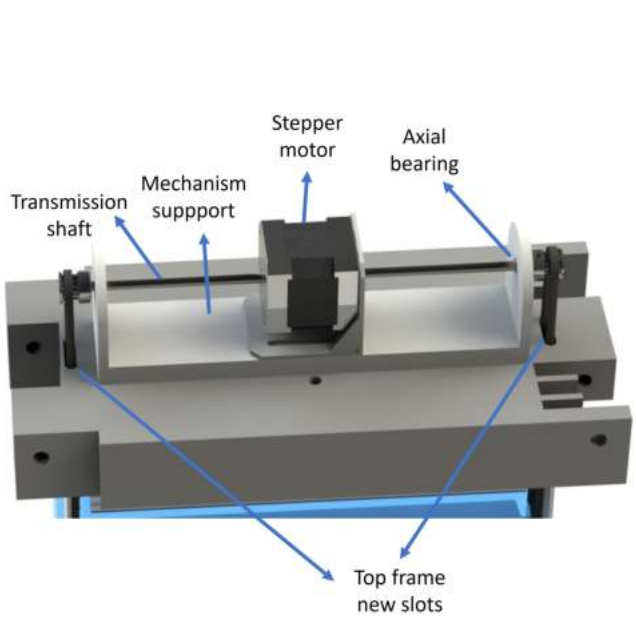

(a) Detail top

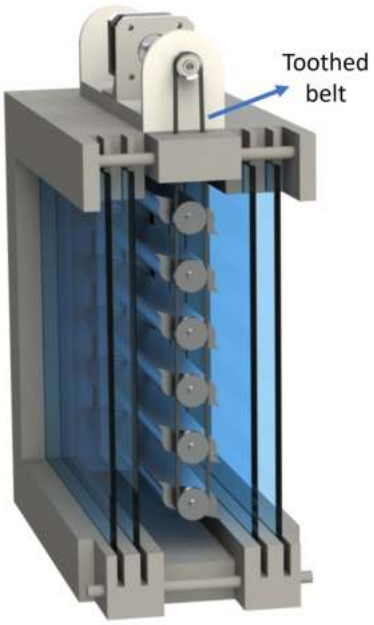

(b) Toothed belt

Figure 4.14: Tilting mechanism details

The slats are driven by the toothed belt, which is connected to its cover. The slats cover shown in figure 4.15a were designed with a spur gear, and a cylindrical guide. The used tilting matrices would be replaced by two holding matrices (figure 4.15b), where the cylindrical guides from the slats cover would fit, allowing the slat to rotate and preventing to drop.

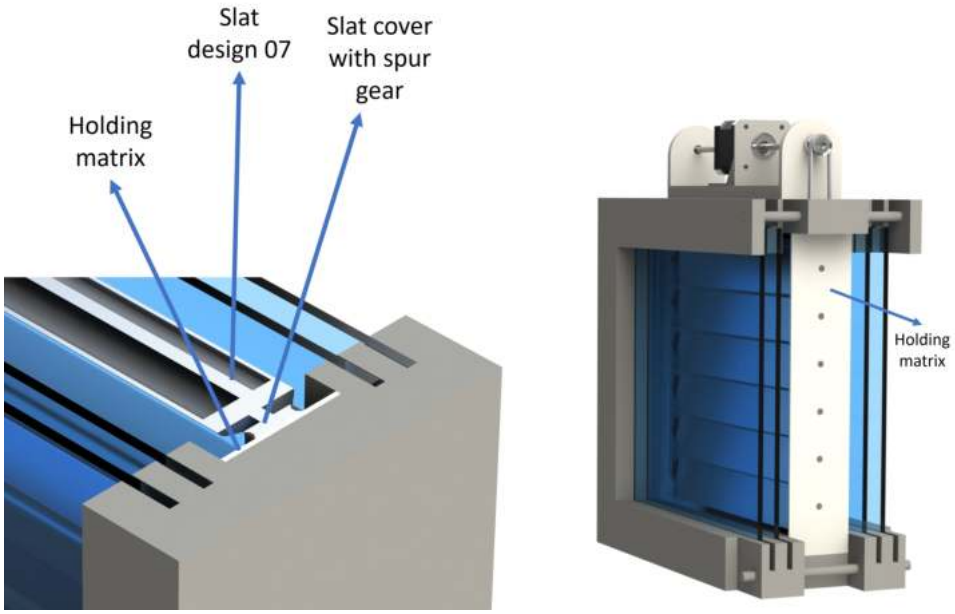

(a) Tilting mechanism - slat detail (b) Holding matrix

Figure 4.15: Tilting mechanism slat details

Besides slats filled with PCM the prototype can be used to evaluate the energy production from slats with PV cells implemented, or evaluate photovoltaic window glass. The prototype can also be used to test intelligent algorithms that improve the efficiency of the slat positions, when working with automatic control systems.

For future detailed analysis of the PCM effect a different approach should be taken when planning the experimental tests methodology. It is important to understand the PCM thermodynamic state inside the slat, and it is important to understand the prototype performance when submitted to solar radiation.

To understand and optimize the thermodynamic behaviour of the PCM inside the slat, computational fluid dynamic simulations (CFD) can be used. CFD are mainly used for solving heat transfer and fluid dynamics problems, and it is an important field to approach in future. Several calculation techniques are used such as finite difference methods, Gauss-Seidel , finite difference, PRESTO algorithm, among others. Several computational tools can be used for the model development, as *MATLAB®* and *ANSYS Fluent* [82]. To get the analysis done, the used instrumentation should be complemented with two heat flux sensors placed on each side of the slat. The proposed analysis would

have the following considerations: uni-dimensional analysis; neglected contact resistances and natural air convection should be considered. The prototype thermal resistance scheme is presented in figure 4.16 and the heat transfer happens through conduction (in the glazing, in the aluminium of the slat and the interior of the slat) and through natural convection (in the air between the solid surfaces).

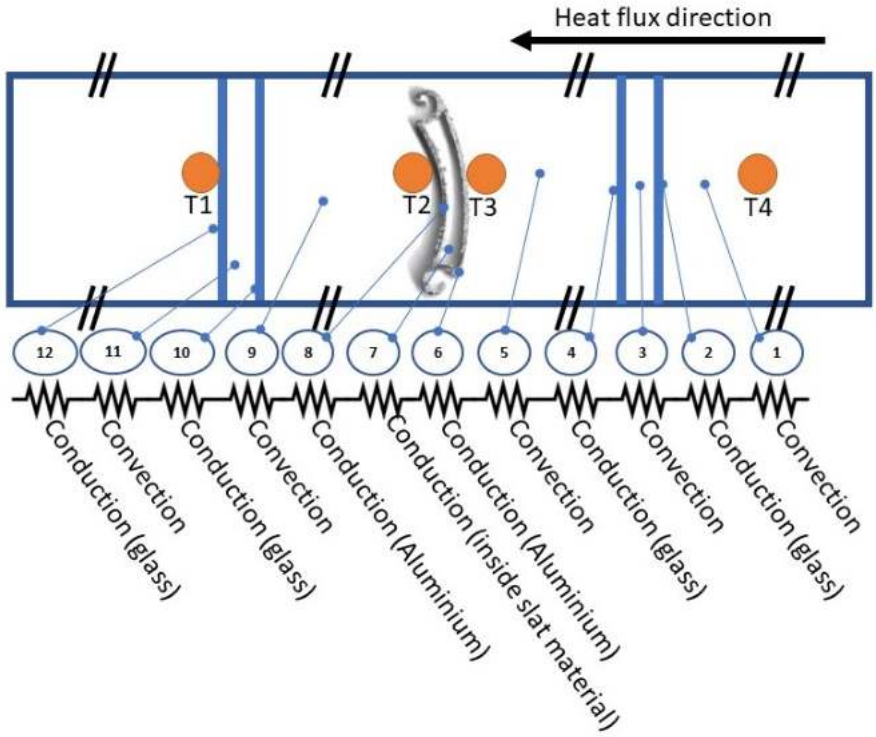

Figure 4.16: Thermal circuit equivalent considering an uni-dimensional analysis

In addition to the numerical modelling of the PCM, optimization techniques can be applied to evaluate and improve its economic and environmental sustainability. The optimization can be done defining objective functions and its limitations from the mathematical model and use machine learning algorithms (Teaching Learning Based Optimization (TLBO), Particle Swarm Optimization (PSO), among others) to solve it [82].

Part III

Conclusion

Chapter 5

Conclusions

In section 1.1 the aim of the project was presented:

> " *This project aims to develop a scaled conceptual prototype of a window blind mechanism that allows the slat to rotate from -90º to +90º with the floor, to direct the layer where it is convenient to reduce room thermal inertia and ventilation systems consumption. It is also aimed to get experimental results of the thermal performance from the PCM inside slats*"

During all the project several challenges were faced. Focusing on the chapter 3 - Prototype development in section 3.2, the first challenges appeared. A slat design was developed, with FDM process, working as a macro capsule for the PCM, which did not work due to PCM leaking problem. An approach was taken to understand the viability of FDM printing process as a macro capsule. An experimentation was made using cups with different printing conditions, which confirmed that FDM process with the used specifications did not guarantee the sealing of the PCM for this specific application. The problem was solved using commercialized aluminium profiles sealed with high temperature silicone, which after the experimental tests did not presented any weight difference.The framing and tilting mechanisms were developed using FDM process. The chosen material was PETg due to its thermal resistance since thermal experimentation was furtherly done. The framing was developed replicating a double glazing surfaces system, using in total, four glass with 4 mm thickness. The developed framing is modular, so it can be easily extended in area. The slat tilting mechanism was developed in form of independent matrices for each tilt angle, which implies the disassembly of the prototype for each tilt angle analysis.

From chapter 4 it was possible to understand the methodology of experimental tests. An instrumentation system was improved in order to monitor remotely the prototype, with the data log being easily available on an online shareable spreadsheet. From the experimental test with open slats matrix it was concluded that no difference was found from a conventional slat to a slat filled with PCM, hence, it is extremely important to understand the user behaviour about the slats position or implement automatic systems.

For the experimental tests with closed slats, three iterations were needed due to lack

of sensibility for the melting temperature. The oven temperature in the first experimental test was not enough for the PCM to reach latent stage, so the temperature was raised 10℃. In the second experimental test, the thermal sensors were stack directly in the slats to avoid air thermal resistance, and the PCM reached the beginning of the melting point. In the last experimental test, the oven temperature was raised another 10℃, which resulted in a fully phase change from material. From this last experimental test, it was now possible to notice the peak shifting due to the phase change of the material. It was possible to understand that, even with a higher thermal conductivity, the slat with PCM remained its temperature under the convectional slat temperature for 4.5 hours, getting the highest temperature difference of -5.13% in the latent phase.

Overall, the project goals were accomplished. A conceptual prototype was developed to test the performance of slats with PCMs. Fast prototyping was a fundamental technology used in the project, allowing the development of a modular prototype that can be easily adapted to test slats filled with different materials.

Being window glazing responsible for 10 to 15% of heat losses in new buildings, this field still have a lot of research to be done. Improving window blind systems thermal efficiency or using it as energy producer (electrical), energy store (thermal), or both, will definitely have an impact in energy demand and consumption.

Part IV

References

References

[1] *Directive 2010/31/eu of the european parliament and of the council of 19 may 2010 on the energy performance of buildings*. (2016).

[2] *The european commission's priorities — european commission*. (2022). https://ec.europa.eu/info/strategy/priorities-2019-2024_en

[3] *A european green deal — european commission*. (2022). https://ec.europa.eu/info/strategy/priorities-2019-2024/european-green-deal_en

[4] Greffet, R., Salagnac, P., Michaux, G., & Ridoret, J.-B. (2013). Airflow window: Numerical study and sensibility analysis of thermal performances. *13th Conference of International Building Performance Simulation Association*.

[5] Visockis, E., Selegovskis, R., & Pleiksnis, S. (2015). Heat losses decreasing possibilities through buildings windows.

[6] D'Agostino, D., Cuniberti, B., & Bertoldi, P. (2017). Energy consumption and efficiency technology measures in european non-residential buildings. *Energy and Buildings*, *153*, 72–86. https://doi.org/10.1016/j.enbuild.2017.07.062

[7] *The history of window blinds - shutter masters*. (2022). https://shuttermasters.com/the-history-of-window-blinds/

[8] Evangelisti, L., Guattari, C., Asdrubali, F., & de Lieto Vollaro, R. (2020). An experimental investigation of the thermal performance of a building solar shading device. *Journal of Building Engineering*, *28*. https://doi.org/10.1016/J.JOBE.2019.101089

[9] Soares, N., Costa, J. J., Gaspar, A. R., & Santos, P. (2013). Review of passive pcm latent heat thermal energy storage systems towards buildings' energy efficiency. *Energy and Buildings*, *59*, 82–103. https://doi.org/10.1016/J.ENBUILD.2012.12.042

[10] *Dgeg ¿ eficiência energécia ¿ edifícios*. (2022). https://www.dgeg.gov.pt/pt/areas-setoriais/energia/eficiencia-energetica/edificios/

[11] Agency, I. E. (2020). *Statistics report key world energy statistics 2020*.

[12] *Shares of residential energy consumption by end use in selected iea countries, 2019 – charts – data and statistics - iea*. (2022). https://www.iea.org/data-and-statistics/charts/shares-of-residential-energy-consumption-by-end-use-in-selected-iea-countries-2019

[13] of Energy, U. D. (2015). *An assessment of energy technologies and research opportunities chapter 5: Increasing efficiency of building systems and technologies*.

[14] D'Agostino, D., Zangheri, P., & Castellazzi, L. (2017). Towards nearly zero energy buildings in europe: A focus on retrofit in non-residential buildings. *Energies 2017, Vol. 10, Page 117*, *10*, 117. https://doi.org/10.3390/EN10010117

[15] *Eu priorities*. (2022). https://european-union.europa.eu/institutions-law-budget/decision-making-process/eu-priorities_en

[16] *Delivering the european green deal — european commission*. (2022). https://ec.europa.eu/info/strategy/priorities-2019-2024/european-green-deal/delivering-european-green-deal_en

[17] *Eu law - eur-lex*. (2022). https://eur-lex.europa.eu/homepage.html

[18] *Eficiência energética nos edifícios -*. (2022). https://www.adene.pt/eficiencia-energetica-nos-edificios/

[19] Naylor, D., Shahid, H., Harrison, S. J., & Oosthuizen, P. H. (2006). A simplified method for modelling the effect of blinds on window thermal performance. *International Journal of Energy Research*, *30*, 471–488. https://doi.org/10.1002/ER.1162

[20] Karjalainen, S. (2019). Be active and consume less—the effect of venetian blind use patterns on energy consumption in single-family houses. *Energy Efficiency*, *12*, 787–801. https://doi.org/10.1007/S12053-018-9693-X

[21] Ali, H., Hayat, N., Farukh, F., Imran, S., Kamran, M. S., & Ali, H. M. (2017). Key design features of multi-vacuum glazing for windows a review. *Thermal Science*, *21*, 2673–2687. https://doi.org/10.2298/TSCI151006051A

[22] Humaish, H. (2018). Evaluate heat loss through windows by using guarded hot box (ghb). *Journal of Physics: Conference Series*, *1032*. https://doi.org/10.1088/1742-6596/1032/1/012025

[23] *Difference between single vs double pane glass windows — pella windows and doors*. (2022). https://www.pellabranch.com/blog/global-blogs/single-vs-double-pane-windows--know-the-difference/

[24] *Ec95 thermeco*. (2022). https://thermeco.com.au/products/aluminium/residential/sliding/window/ec95-2/

[25] *Single pane vs double pane windows*. (2022). https://wanjiadw.com/single-pane-vs-double-pane-windows/

[26] Kirimtat, A., Koyunbaba, B. K., Chatzikonstantinou, I., & Sariyildiz, S. (2016). Review of simulation modeling for shading devices in buildings [survey of simulation tools]. *Renewable and Sustainable Energy Reviews*, *53*, 23–49. https://doi.org/10.1016/J.RSER.2015.08.020

[27] *Beautiful free images and pictures — unsplash*. (2022). https://unsplash.com/

[28] *Roller shutters — modern roller shutters for windows and doors*. (2022). https://www.halfpriceshutters.com.au/roller-shutters/#1601283502944-8cded3c5-6a70

[29] *Sk, ske and skp front mounted roller shutters — aluprof sa*. (2022). https://www.rolety.aluprof.eu/en/system-sk

[30] *Traditional french pinoleum blinds for conservatories and orangeries — grants blinds*. (2022). https://www.grantsblinds.com/traditional-french-pinoleum-blinds

[31] *Lowe's home improvement*. (2022). https://www.lowes.com/

[32] *Origin, soft white - day night blind — 247blinds.* (2022). https://www.247blinds.co.uk/origin-soft-white-day-night-blind

[33] *Estores de clarabóia para roto r85 5/7 - jet black blackout, opaco - basic — ouro estores.* (2022). https://www.ouroestores.pt/sobre/cortinas/roto/R85WOOD/5_7/2228-228?gclid=Cj0KCQjwio6XBhCMARIsAC0u9aH_BAg2l8Vm7ADcszZ-NhivAQAAlLcVyok9UV-_8W_I_X0vLTdP6SUaArNLEALw_wcB

[34] *Ziptrak blind - the curtain boutique - blinds and curtains singapore.* (2022). https://www.tcb.com.sg/ziptrak-singapore/

[35] *Serena light pvc roller shutter 4,5 kg/mq — windowo.* (2022). https://www.windowo.com/pvc-roller-shutter-serena-pinto

[36] *Bamboo horizontal chick blind, rs 120/square feet rivora and co. — id: 17094621762.* (2022). https://www.indiamart.com/proddetail/bamboo-chick-blind-17094621762.html

[37] *Brookstone-total-blackout-eyelet-curtains.* (2022). https://www.costco.co.uk/Furniture-Mattresses/Home-Furnishings-Accessories/Home-Decor/Brookstone-Total-Blackout-Eyelet-Curtains-228-x-228-cm-in-Grey/p/3458321

[38] *444 tellow photos - free and royalty-free stock photos from dreamstime.* (2022). https://www.dreamstime.com/photos-images/tellow.html

[39] *Buy argos home vertical blind pack - white — blinds — argos.* (2022). https://www.argos.co.uk/product/4359582

[40] Gomes, M. G., Santos, A. J., & Rodrigues, A. M. (2014). Solar and visible optical properties of glazing systems with venetian blinds: Numerical, experimental and blind control study. *Building and Environment*, *71*, 47–59. https://doi.org/10.1016/J.BUILDENV.2013.09.003

[41] Hong, S., Choi, A. S., & Sung, M. (2017). Development and verification of a slat control method for a bi-directional pv blind. *Applied Energy*, *206*, 1321–1333. https://doi.org/10.1016/J.APENERGY.2017.10.009

[42] Tzempelikos, A. (2008). The impact of venetian blind geometry and tilt angle on view, direct light transmission and interior illuminance. *Solar Energy*, *82*, 1172–1191. https://doi.org/10.1016/J.SOLENER.2008.05.014

[43] *Integral blind options - midland bi-folds uk.* (2022). https://www.midlandbifolds.co.uk/integral-blind-options/

[44] *Bi design blinds.* (2022). https://www.bidesignblinds.com/

[45] *Pros and cons of honeycomb shades — a little design help.* (2022). http://alittledesignhelp.com/pros-and-cons-of-honeycomb-shades/

[46] Karpouzas, H. (2003). *A casa moderna ocidental e o japão: A influência da arquitetura tradicional japonesa na arquitetura das casas modernas ocidentais.*

[47] *Shoji screens.* (2022). http://www.rothteien.com/superbait/shojiscreens.htm

[48] *A look at quality.* (2022). https://www.retractableawnings.com/university/a-look-at-quality/

[49] *Amazon.com: Chicology cordless cellular shades privacy single cell window blind, 30" w x 64" h, morning ocean light filtering - ccsmo3064 : Home and kitchen.* (2022). https://www.amazon.com/Chicology-Cordless-Cellular-Privacy-Filtering/

dp/B075KZXRVG/ref=sr_1_1?crid=1LRTEF06N6VBE&keywords=Chicology+Shades+celular&qid=1659108491&sprefix=chicology+shades+ce%2Caps%2C2655&sr=8-1

[50] *Stock images, royalty-free pictures, illustrations and videos - istock*. (2022). https://www.istockphoto.com/

[51] *Windsor shoji blinds - contemporary - living room - other - by highbury design ltd — houzz ie*. (2022). https://www.houzz.ie/photos/windsor-shoji-blinds-phvw-vp~13075895

[52] *Mosquito nets made of carbon fiber — insects protection*. (2022). https://www.dakowindows.com/en/products/mosquito-nets

[53] *Windowshade folding arm awning grey*. (2022). https://www.spotlightstores.com/blinds/outdoor-blinds-shades/windowshade-folding-arm-awning/BP80484511-grey

[54] Braun, E., & In, B. S. (1981). *Survey of window-treatment-use among cities with different heating and cooling requirements*.

[55] Yazicioglu, F. (2013). A comparative analysis of the energy performance of traditional wooden shutters and contemporary aluminium roller shutters in istanbul, a case study. *Energy Procedia*, *42*, 483–492. https://doi.org/10.1016/J.EGYPRO.2013.11.049

[56] Wright, J. L., Kotey, N. A., Barnaby, C. S., & Collins, M. R. (2009). Solar gain through windows with shading devices: Simulation versus measurement. https://uwspace.uwaterloo.ca/handle/10012/11596

[57] Cárdenas-Ramírez, C., Jaramillo, F., & Gómez, M. (2020). Systematic review of encapsulation and shape-stabilization of phase change materials. *Journal of Energy Storage*, *30*. https://doi.org/10.1016/J.EST.2020.101495

[58] Khan, Z., Khan, Z., & Ghafoor, A. (2016). A review of performance enhancement of pcm based latent heat storage system within the context of materials, thermal stability and compatibility. *Energy Conversion and Management*, *115*, 132–158. https://doi.org/10.1016/J.ENCONMAN.2016.02.045

[59] Sivanathan, A., Dou, Q., Wang, Y., Li, Y., Corker, J., Zhou, Y., & Fan, M. (2020). Phase change materials for building construction: An overview of nano-/micro-encapsulation. *Nanotechnology Reviews*, *9*, 896–921. https://doi.org/10.1515/ntrev-2020-0067

[60] Cabeza, L. F., Ibáñez, M., Solé, C., Roca, J., & Nogués, M. (2006). Experimentation with a water tank including a pcm module. *Solar Energy Materials and Solar Cells*, *90*, 1273–1282. https://doi.org/10.1016/j.solmat.2005.08.002

[61] Benchara, E. H., Jennah, S., Belouggadia, N., Mansouri, K., & Bouattane, O. (2020). Thermal energy storage by phase change materials suitable for solar water heaters: An updated review. *2020 IEEE 2nd International Conference on Electronics, Control, Optimization and Computer Science, ICECOCS 2020*. https://doi.org/10.1109/ICECOCS50124.2020.9314561

[62] Akeiber, H. J., Wahid, M. A., Hussen, H. M., & Mohammad, A. T. (2014). Review of development survey of phase change material models in building applications. *Scientific World Journal*, *2014*. https://doi.org/10.1155/2014/391690

[63] Xu, B., Li, P., & Chan, C. (2015). Application of phase change materials for thermal energy storage in concentrated solar thermal power plants: A review to recent developments. *Applied Energy*, *160*, 286–307. https://doi.org/10.1016/J.APENERGY.2015.09.016

[64] Bashir, M. A., Giovannelli, A., Amber, K. P., Khan, M. S., Arshad, A., & Daboo, A. M. (2020). High-temperature phase change materials for short-term thermal energy storage in the solar receiver: Selection and analysis. *Journal of Energy Storage*, *30*. https://doi.org/10.1016/J.EST.2020.101496

[65] Vicente, R., & Silva, T. (2014). Brick masonry walls with pcm macrocapsules: An experimental approach. *Applied Thermal Engineering*, *67*, 24–34. https://doi.org/10.1016/j.applthermaleng.2014.02.069

[66] Wang, H., Lu, W., Wu, Z., & Zhang, G. (2020). Parametric analysis of applying pcm wallboards for energy saving in high-rise lightweight buildings in shanghai. *Renewable Energy*, *145*, 52–64. https://doi.org/10.1016/j.renene.2019.05.124

[67] Li, Y., Zhou, J., Long, E., & Meng, X. (2018). Experimental study on thermal performance improvement of building envelopes by integrating with phase change material in an intermittently heated room. *Sustainable Cities and Society*, *38*, 607–615. https://doi.org/10.1016/J.SCS.2018.01.040

[68] Youngblood, N., Talagrand, C., Porter, B. F., Galante, C. G., Kneepkens, S., Triggs, G., Sarwat, S. G., Yarmolich, D., Bonilla, R. S., Hosseini, P., Taylor, R. A., & Bhaskaran, H. (2021). Reconfigurable low-emissivity optical coating using ultrathin phase change materials. *ACS Photonics*, acsphotonics.1c01128. https://doi.org/10.1021/ACSPHOTONICS.1C01128

[69] Li, D., Wu, Y., Wang, B., Liu, C., & Arıcı, M. (2020). Optical and thermal performance of glazing units containing pcm in buildings: A review. *Construction and Building Materials*, *233*. https://doi.org/10.1016/J.CONBUILDMAT.2019.117327

[70] Soares, N., Gaspar, A. R., Santos, P., & Costa, J. J. (2016). Experimental evaluation of the heat transfer through small pcm-based thermal energy storage units for building applications. *Energy and Buildings*, *116*, 18–34. https://doi.org/10.1016/J.ENBUILD.2016.01.003

[71] Weinlaeder, H., Koerner, W., & Heidenfelder, M. (2011). Monitoring results of an interior sun protection system with integrated latent heat storage. *Energy and Buildings*, *43*, 2468–2475. https://doi.org/10.1016/J.ENBUILD.2011.06.007

[72] Musiał, M. (2018). Evaluation of the energy efficiency of an internal blind containing pcm. *E3S Web of Conferences*, *49*. https://doi.org/10.1051/e3sconf/20184900074

[73] Silva, T., Vicente, R., Rodrigues, F., Samagaio, A., & Cardoso, C. (2015). Performance of a window shutter with phase change material under summer mediterranean climate conditions. *Applied Thermal Engineering*, *84*, 246–256. https://doi.org/10.1016/J.APPLTHERMALENG.2015.03.059

[74] Hu, H., Jin, X., & Zhang, X. (2017). Effect of supercooling on the solidification process of the phase change material. *Energy Procedia*, *105*, 4321–4327. https://doi.org/10.1016/J.EGYPRO.2017.03.905

[75] Relvas, C. (2017). *O mundo da impressão e o fabrico digital*. www.engebook.com

[76] Attaran, M. (2017). The rise of 3-d printing: The advantages of additive manufacturing over traditional manufacturing. *Business Horizons*, *60*, 677–688. https://doi.org/10.1016/j.bushor.2017.05.011

[77] *Tucab*. (2022). https://www.tucab.pt/

[78] *Energy technologies*. (2022). https://www.crodaenergytechnologies.com/en-gb

[79] *Instrumentos testo s.a. — soluções e instrumentos de medição*. (2022). https://www.testo.com/pt-PT/

[80] Santos, C. A. P., & Matias, L. (2009). Coeficientes de transmissão térmica de elementos da envolvente dos edifícios., 170. https://www.booki.pt/loja/prod/ite-50-coef-de-transmissao-termica-de-elementos-da-envolvente-dos-edificios/9789724920658/

[81] Bergman, T. L., Lavine, A. S., Incropera, F. P., & Dewitt, D. P. (2011). Fundamentals of heat and mass transfebergman, t. l., lavine, a. s., incropera, f. p., and dewitt, d. p. (2011). fundamentals of heat and mass transfer. 7th edition. http://doi.org/10.1007/s13398-014-0173-7.2r. 7th edition, 1048.

[82] Goia, F., Perino, M., & Haase, M. (2012). A numerical model to evaluate the thermal behaviour of pcm glazing system configurations. *Energy and Buildings*, *54*, 141–153. https://doi.org/10.1016/j.enbuild.2012.07.036

Part V

Appendix

Appendix A

Prototype technical draws

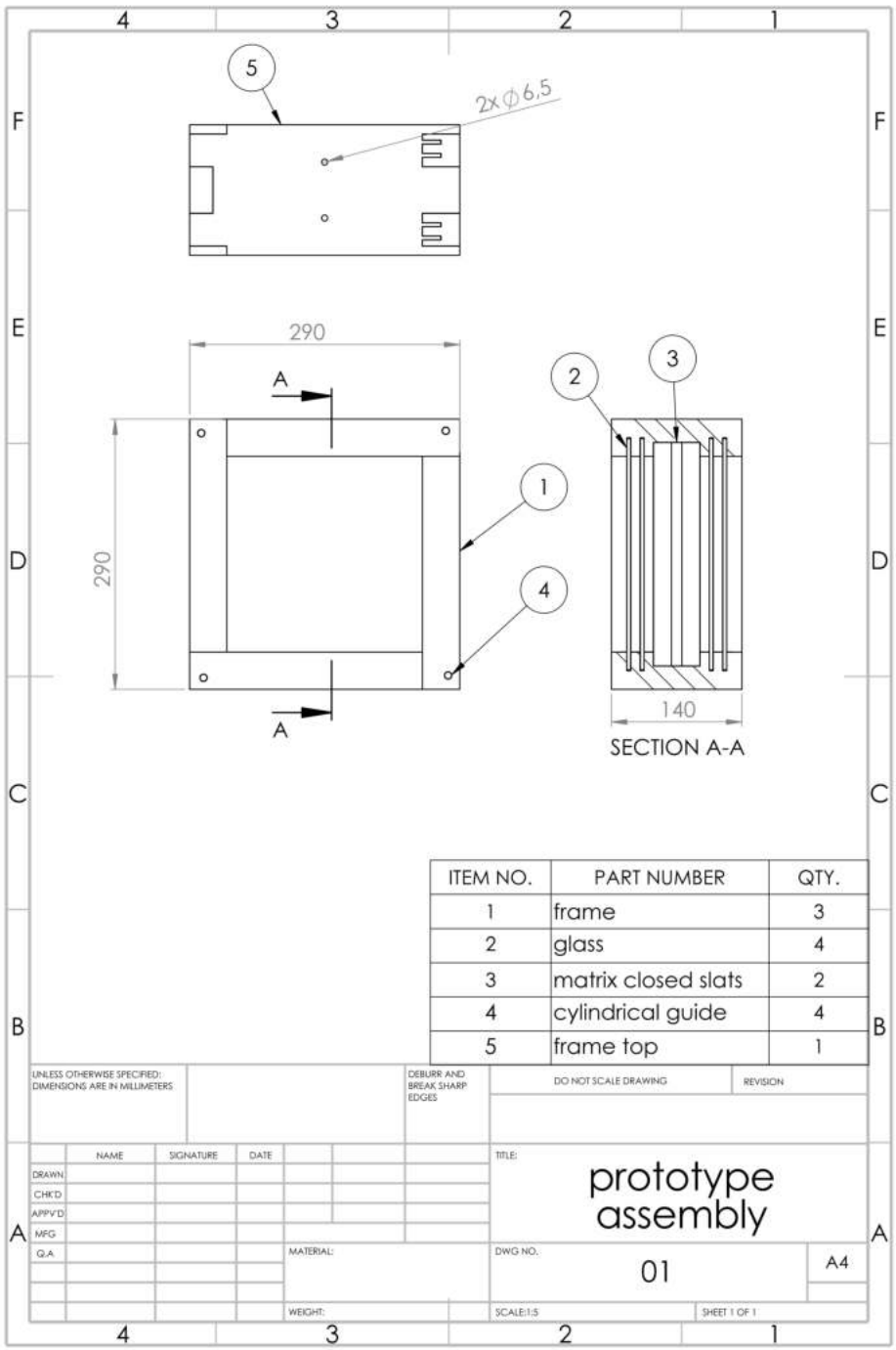

Figure A.1: Draw 01 - Prototype assembly

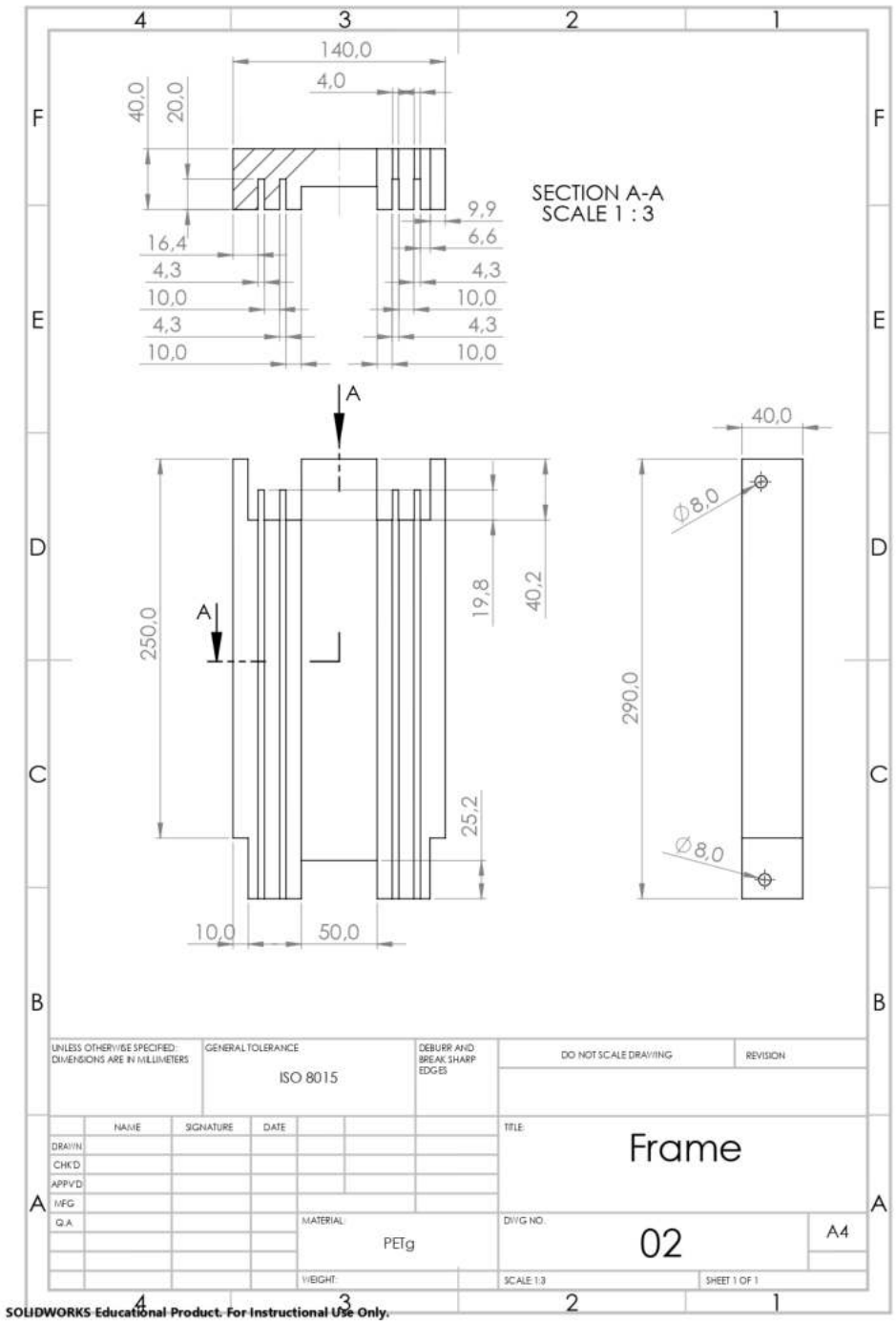

Figure A.2: Draw 02 - Frame

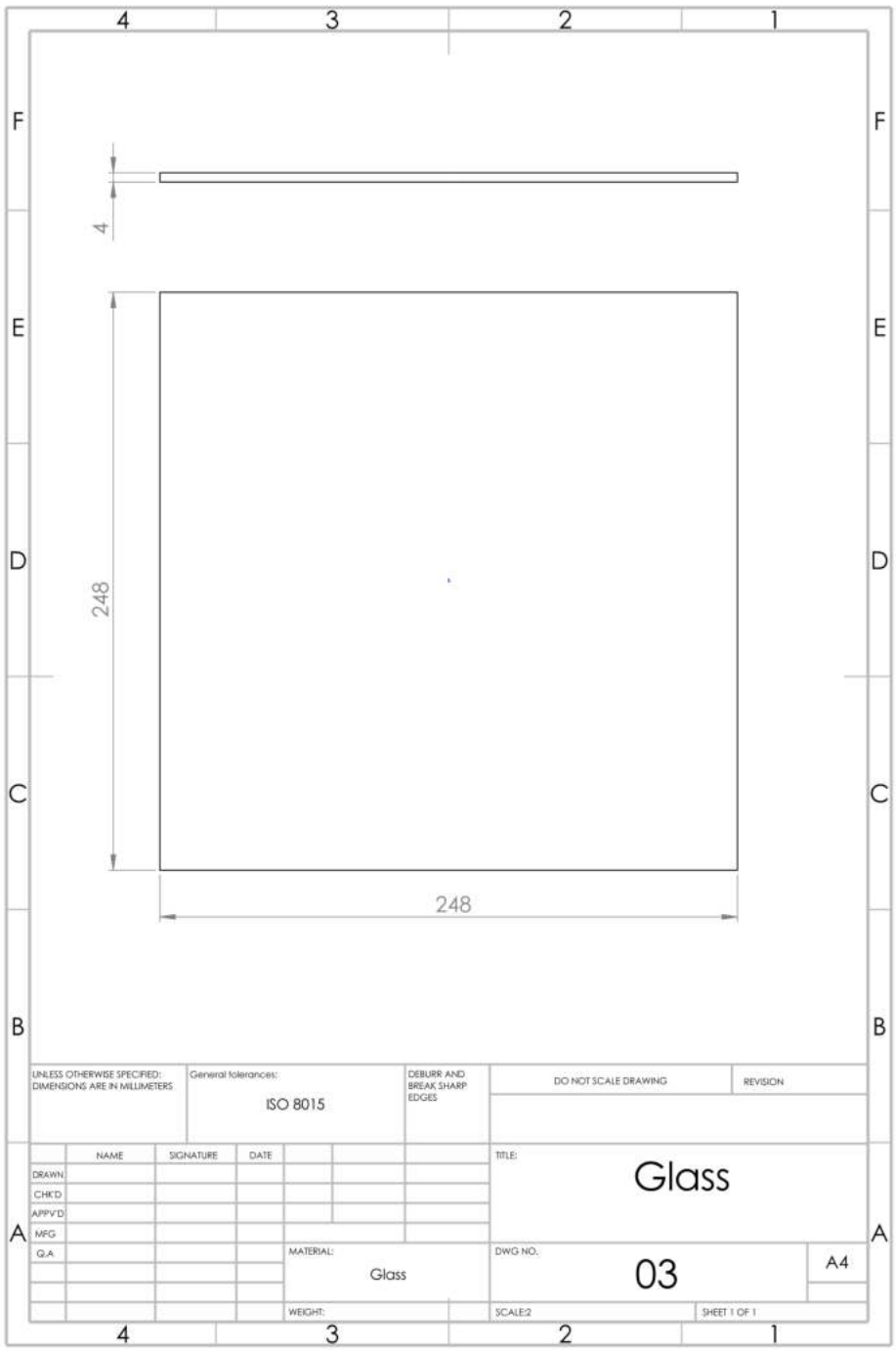

Figure A.3: Draw 03 - Glass

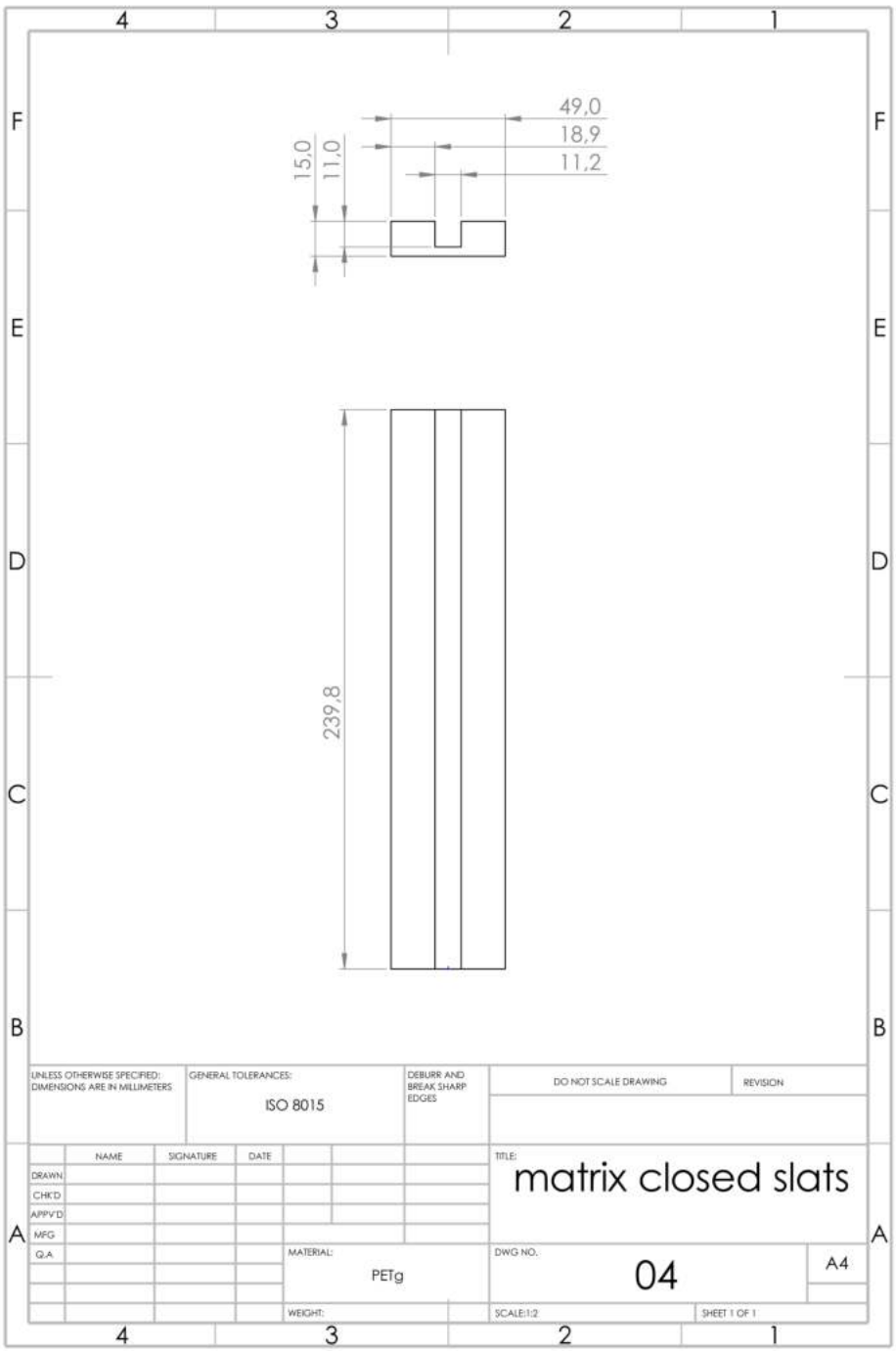

Figure A.4: Draw 04 - Matrix slats 0°

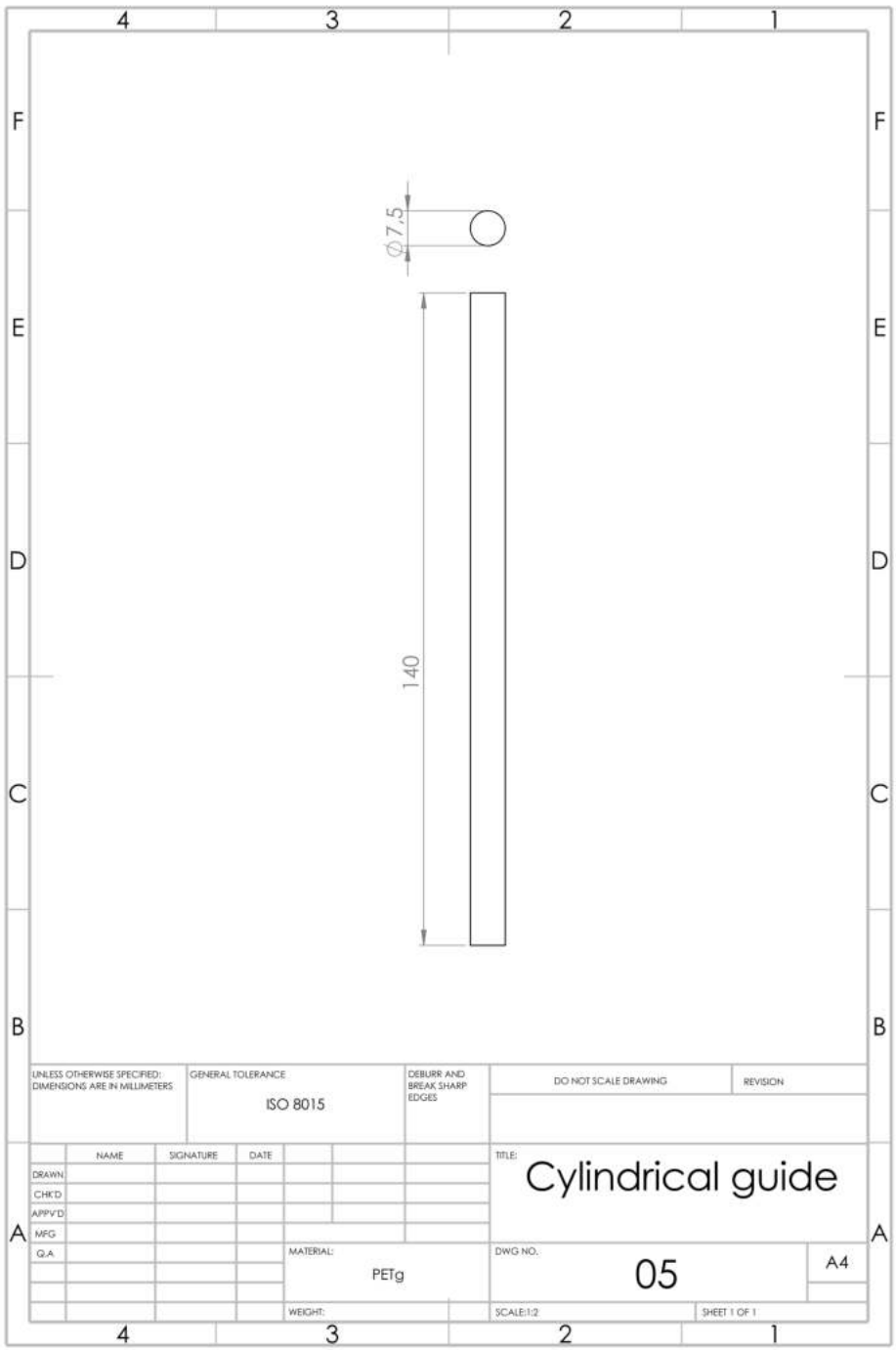

Figure A.5: Draw 05 - Cylindrical guide

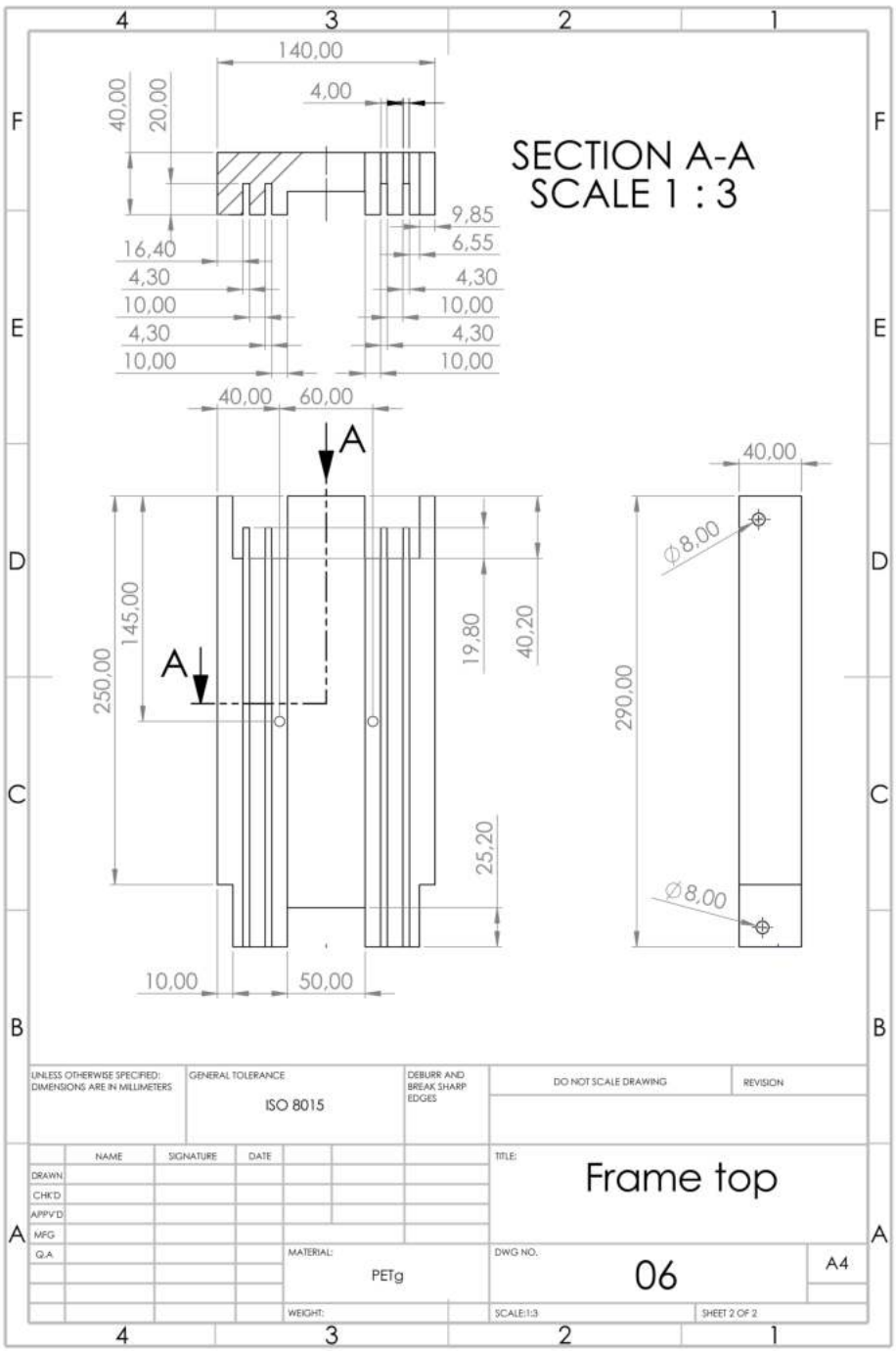

Figure A.6: Draw 06 - Frame top

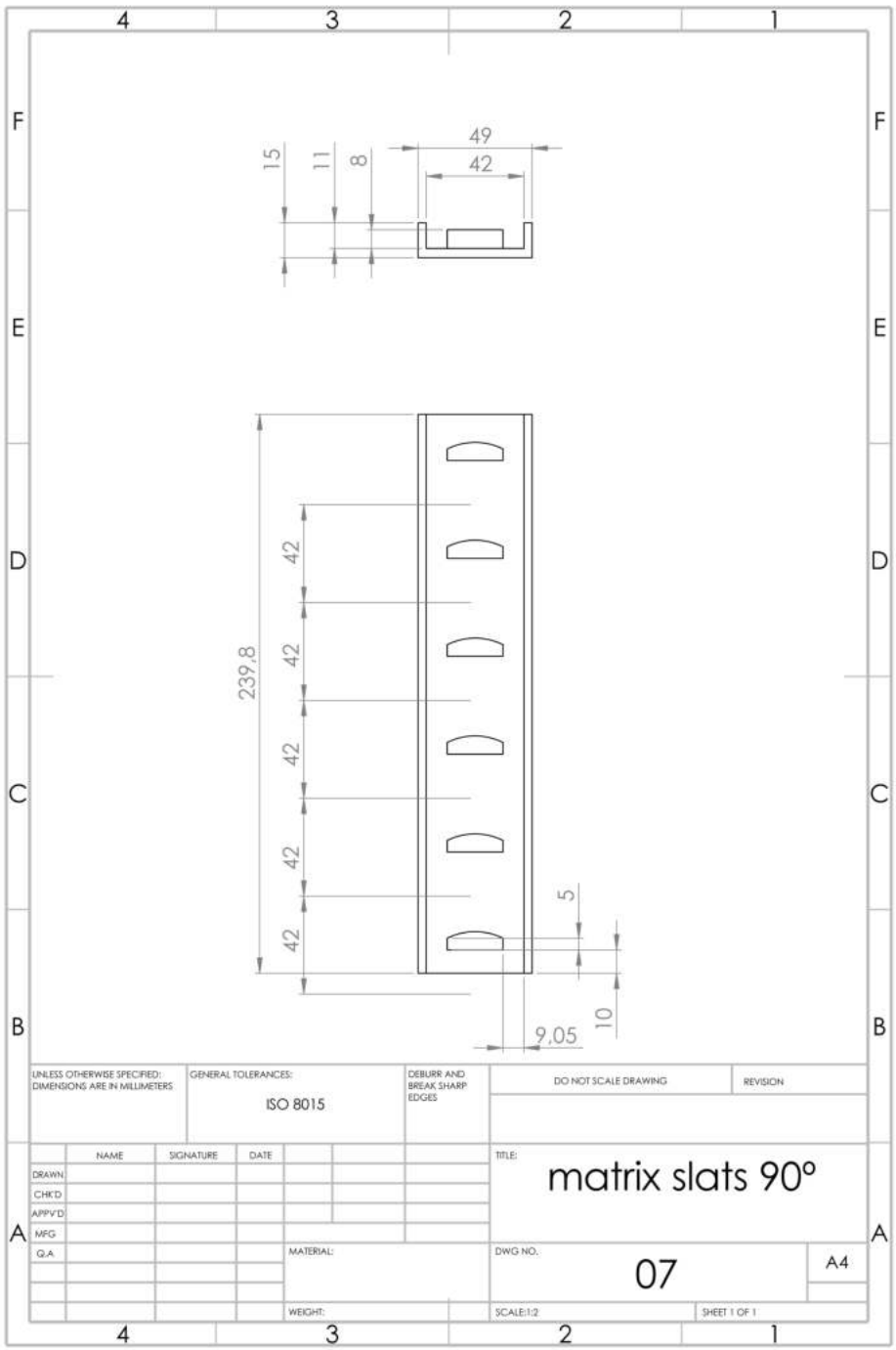

Figure A.7: Draw 07 - Matrix slats 90°

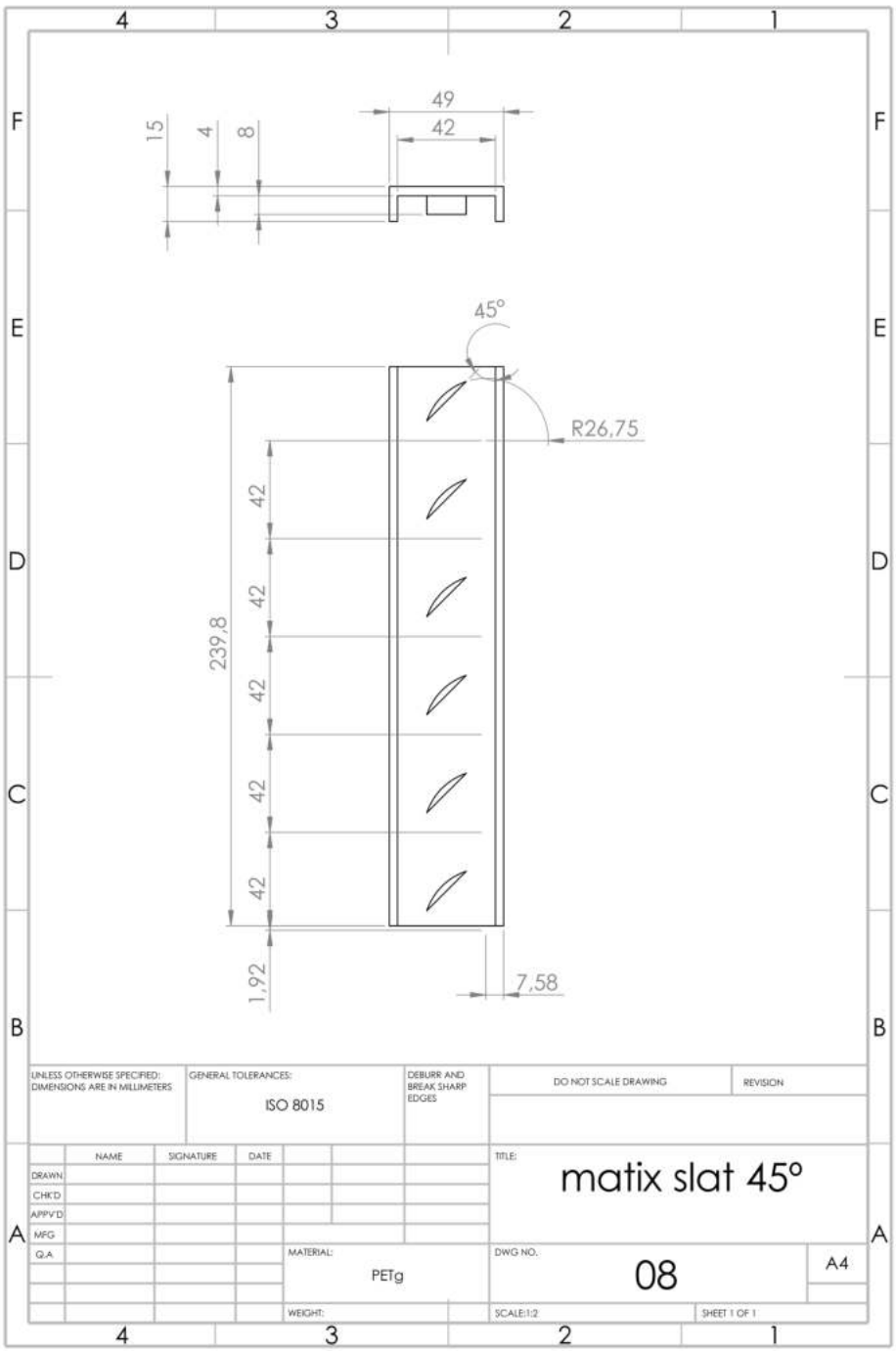

Figure A.8: Draw 08 - Matrix slats 45°

Intentionally blank page.

Appendix B

Laboratory procedure

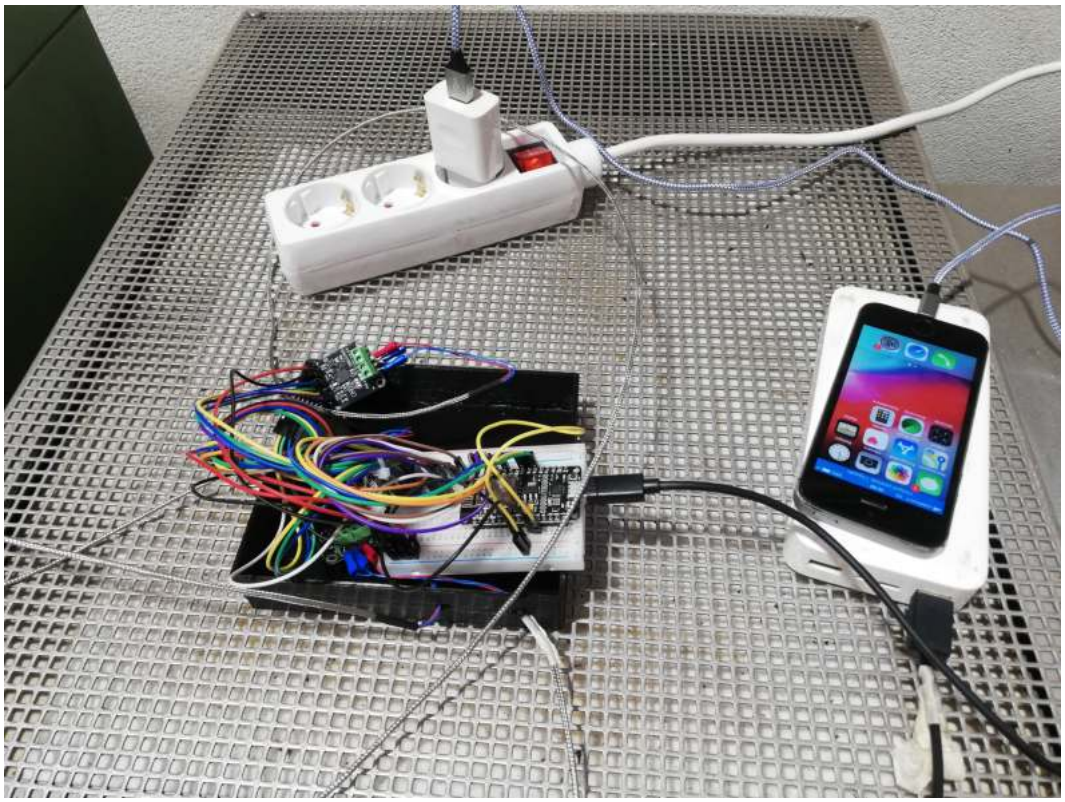

Figure B.1: Instrumentation apparatus

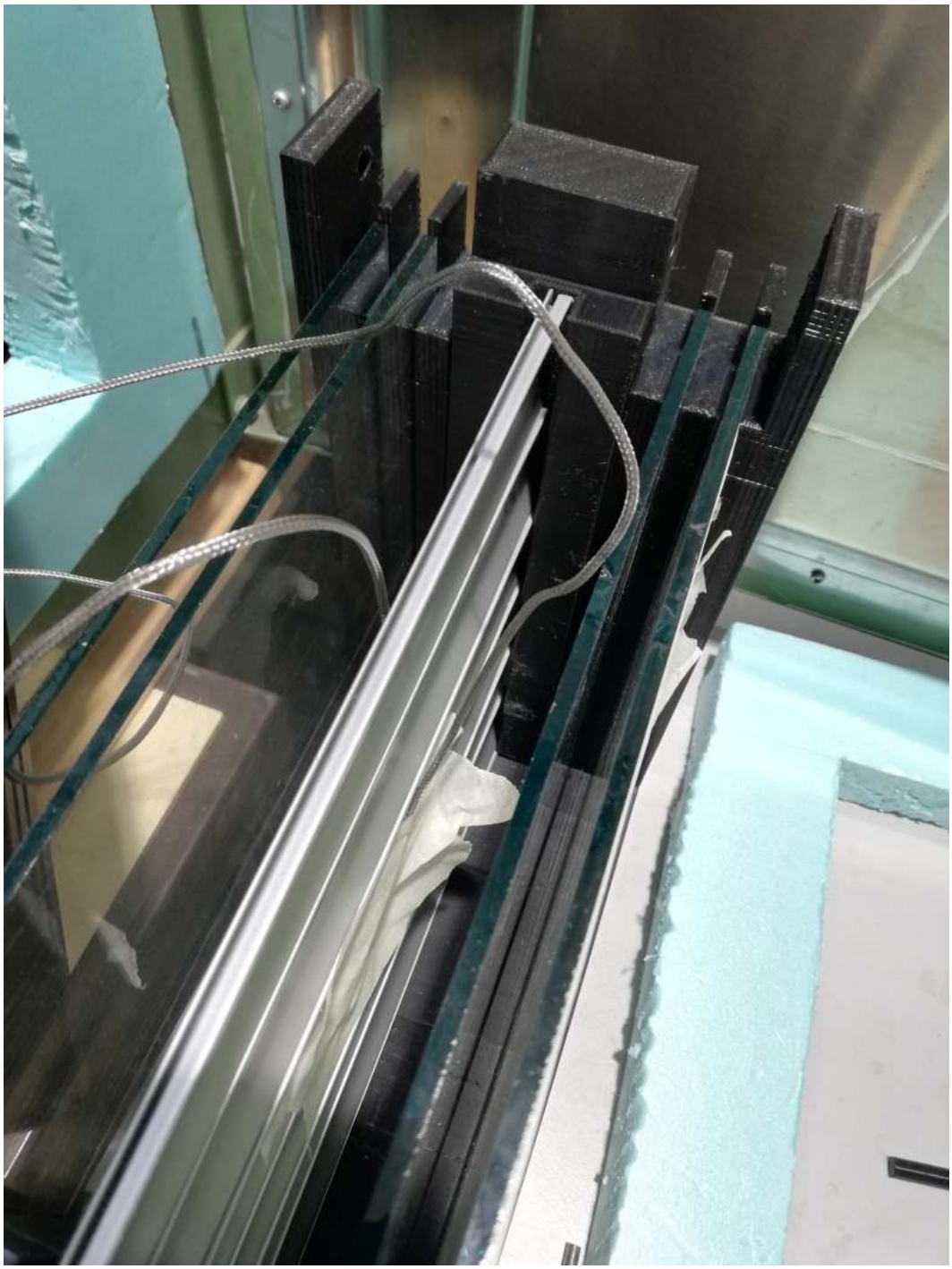

Figure B.2: PT100 stack in slats

Intentionally blank page.

Appendix C

Data from thermographic camera

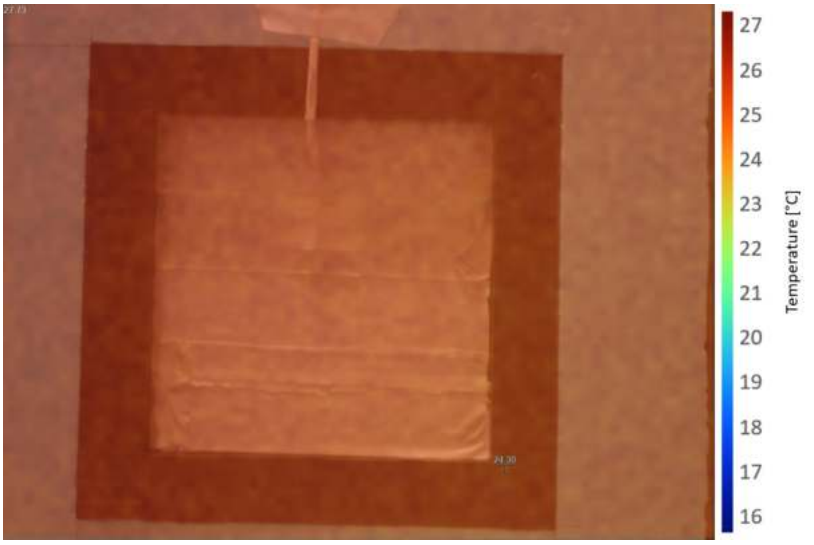

(a) Beginning of experimental test

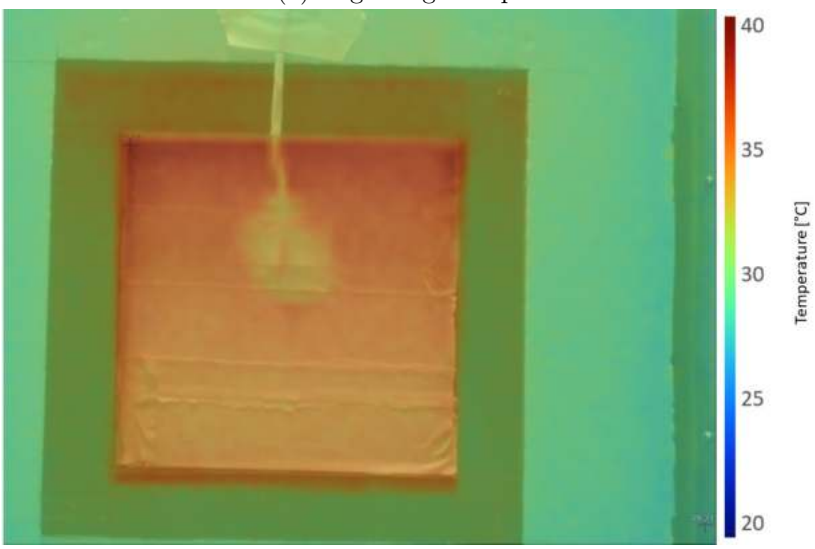

(b) End of experimental test

Figure C.1: Closed conventional 01 slats - thermographic camera

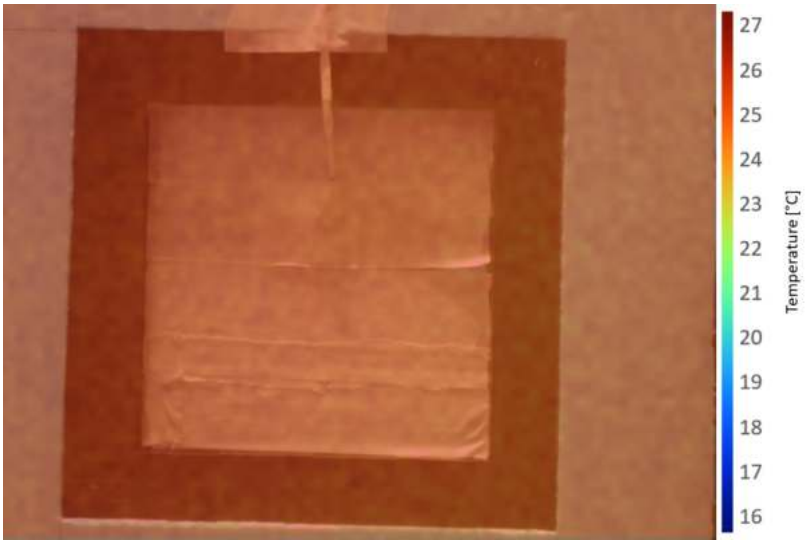

(a) Beginning of experimental test

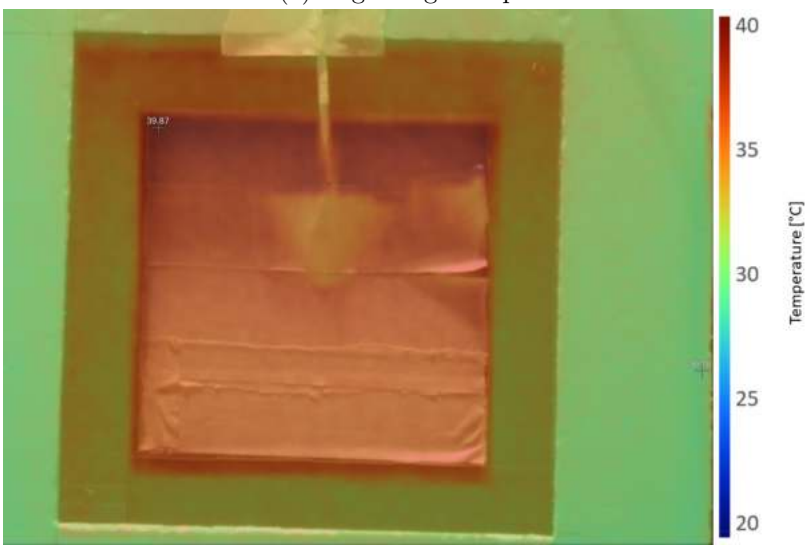

(b) End of experimental test

Figure C.2: Closed slats 01 with PCM - thermographic camera

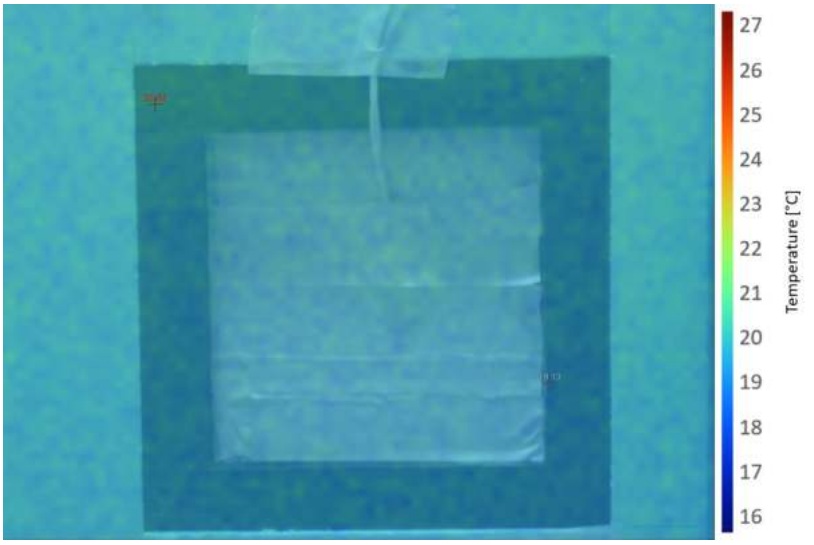

(a) Beginning of experimental test

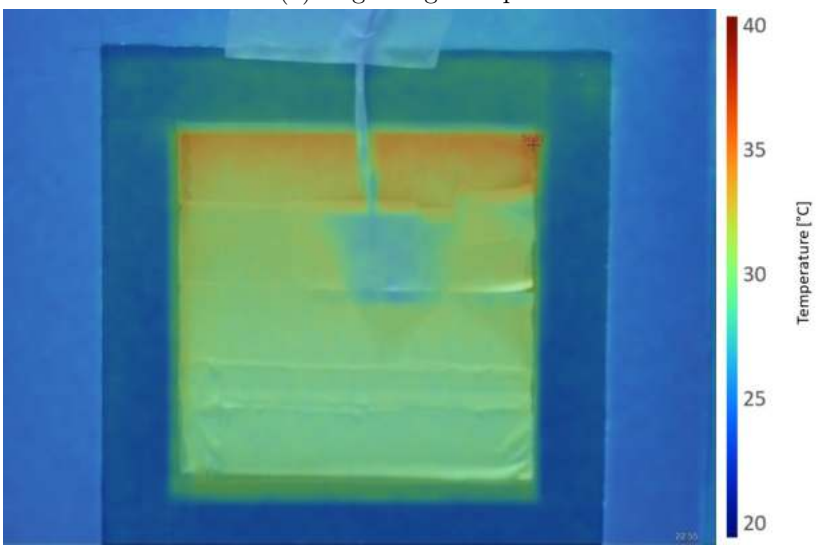

(b) End of experimental test

Figure C.3: Closed slats 02 with PCM - thermographic camera

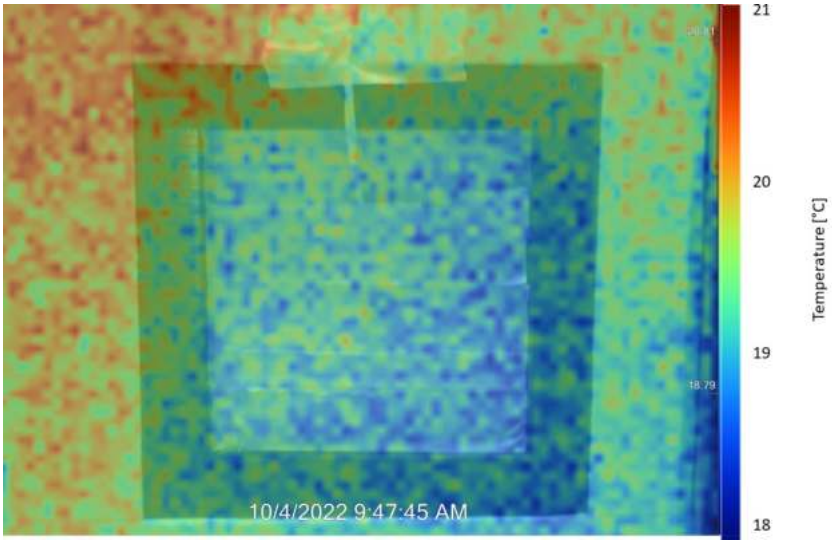

(a) Beginning of experimental test

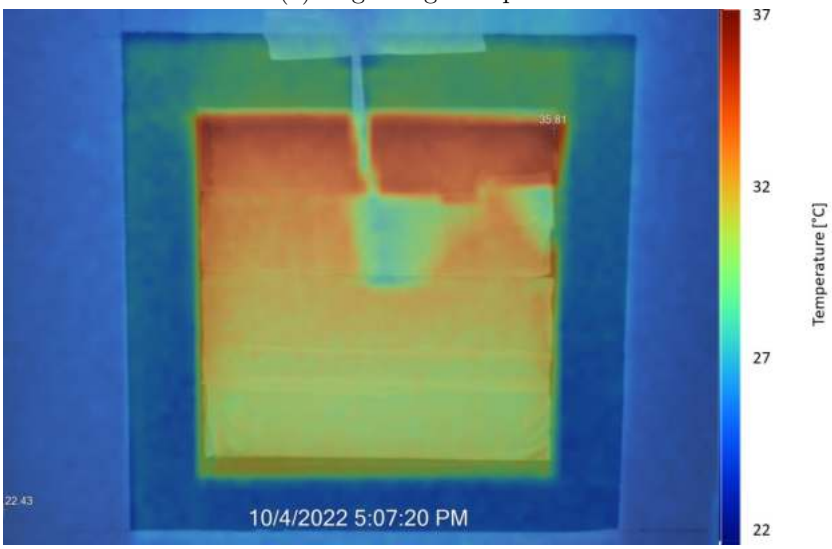

(b) End of experimental test

Figure C.4: Closed conventional 02 slats - thermographic camera

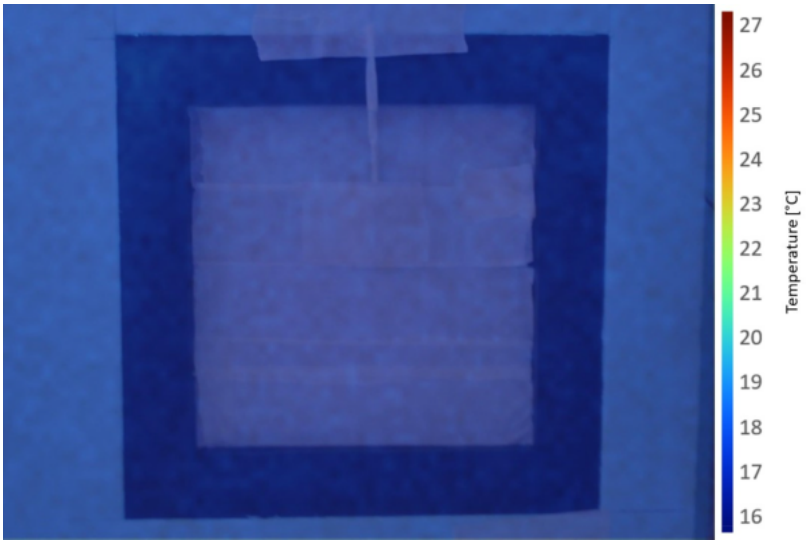

(a) Beginning of experimental test

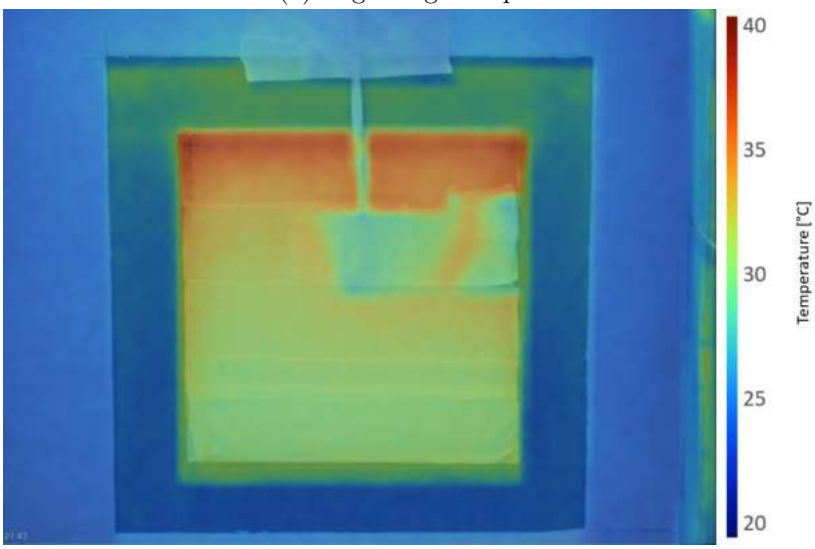

(b) End of experimental test

Figure C.5: Closed slats 03 with PCM - thermographic camera

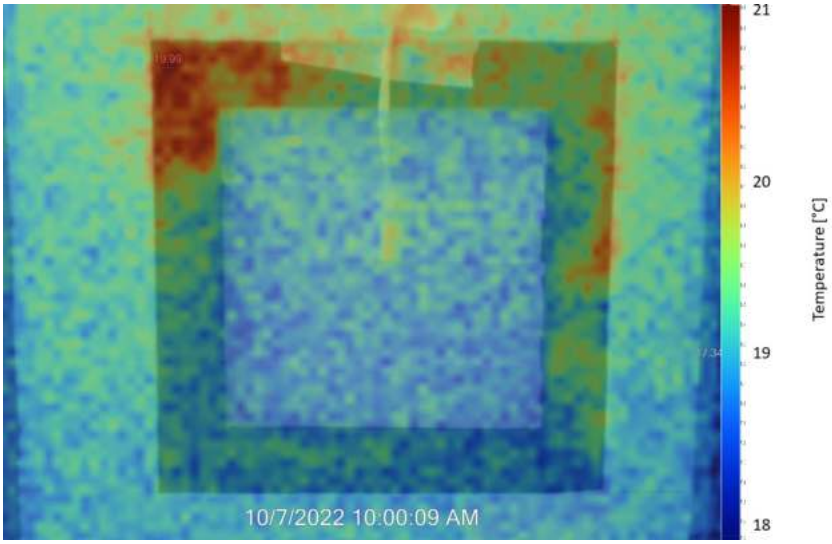

(a) Beginning of experimental test

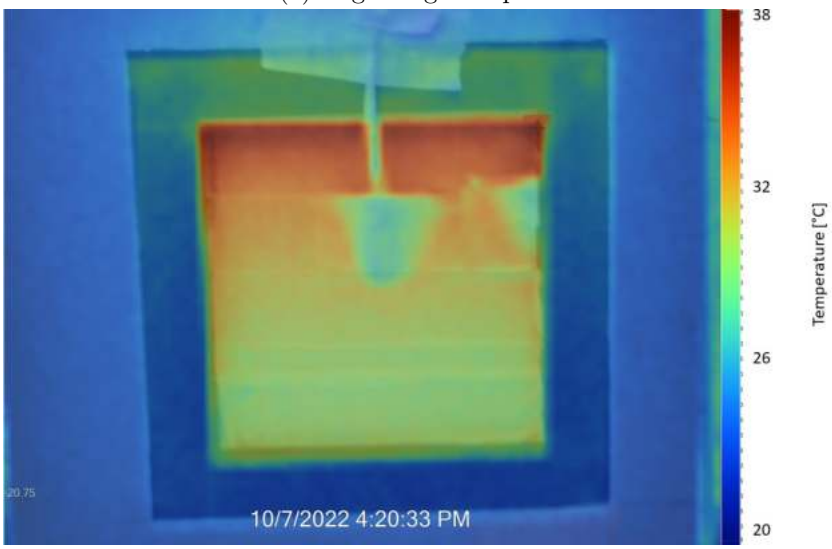

(b) End of experimental test

Figure C.6: Closed conventional 03 slats - thermographic camera